Quantifying the effect of the Drake Passage opening on the Eocene Ocean

A. Toumoulin[1], Y. Donnadieu[1], J.-B. Ladant[2], S. J. Batenburg[3], F. Poblete[4] and G. Dupont-Nivet[3,4,5]

[1]Aix Marseille Université, CNRS, IRD, INRA, Collège de France, CEREGE, Aix-en-Provence, France

[2] Department of Earth and Environmental Sciences, University of Michigan, Ann Arbor, USA.

[3] Géosciences Rennes, UMR CNRS 6118, Univ Rennes, 35000 Rennes, France.

[4] Universidad de Chile, Departamento de Geología, Santiago, Chile.

[5] Institute of Geosciences, Potsdam University, Potsdam, Germany.

Key Points:

- A shallow opening of the Drake Passage induces strong changes in ocean properties and dynamics
- A proto-ACC is able to form during the Eocene under high levels of $p\mathrm{CO_2}$ but a strong ACC requires supplementary geographical changes.
- North Atlantic Deep Water is probably not able to form before the separation of the Arctic and Atlantic Oceans.

Corresponding authors: agathe.toumoulin@gmail.com, donnadieu@cerege.fr

Abstract

The opening of the Drake Passage (DP) during the Cenozoic is a tectonic event of paramount importance for the development of modern ocean characteristics. Notably, it has been suggested that it exerts a primary role in the onset of the Antarctic Circumpolar Current formation (ACC), in the cooling of high-latitude South Atlantic waters and in the initiation of North Atlantic Deep Water (NADW) formation.

Several model studies have aimed to assess the impacts of DP opening on climate, but most of them focused on surface climate and only few used realistic Eocene boundary conditions. Here, we revisit the impact of the DP opening on ocean circulation with the IPSL-CM5A2 Earth System Model. Using appropriate middle Eocene (40 Ma) boundary conditions, we perform and analyze simulations with different depths of the DP (0 m, 100 m, 1000 m and 2500 m) and compare results to existing geochemical data. Our experiments show that DP opening has a strong effect on Eocene ocean structure and dynamics even for shallow depths. The DP opening notably allows the formation of a proto-ACC and induces deep ocean cooling of 1.5°C to 2.5°C in most of the Southern Hemisphere. There is no NADW formation in our simulations regardless of the depth of the DP, suggesting that the DP on its own is not a primary control of deep-water formation in the North Atlantic. This study elucidates how and to what extent the opening of the Drake Passage contributed to the establishment of the modern global thermohaline circulation.

1. Introduction

The Eocene (56 to 33.9 Ma) was a greenhouse period that witnessed major changes in global climate and ocean characteristics (*e.g.* Borrelli *et al.*, 2014; Katz *et al.*, 2011; Pagani *et al.*, 2014). Notably, it is characterized by a long-term gradual cooling initiated by ca 50 Ma, which led to the formation of an ice sheet over Antarctica at the Eocene-Oligocene Transition (EOT; ca 34 Ma) (Zachos *et al.*, 2001). Understanding the cause of this cooling is crucially important to identify governing mechanisms of global climate in relation to geochemical cycles and oceanic circulation. Several tectonic changes occurred during the Eocene, including the Drake Passage (DP) and the Tasmanian Gateway opening, the collision of India and Asia, the narrowing of the Tethys Ocean and the widening of the Atlantic basin (Bice *et al.*, 2000). In particular, the role of DP opening on Eocene cooling has been extensively studied (*e.g.* Elsworth *et al.*, 2017; Goldner *et al.*, 2014; Inglis *et al.*, 2015; Lefebvre *et al.*, 2012; Mikolajewicz *et al.*, 1993; Nong *et al.*, 2000; Sijp & England, 2004; Zhang *et al.*, 2010). It has long been hypothesized that, as it allows the formation of the ACC, DP opening may have induced a thermal isolation of Antarctica and subsequent changes in ocean temperatures (Kennett, 1977). Some model studies have shown that the effect of the DP opening was not sufficient to match the global cooling observed throughout the Eocene. They rather suggest that an additional decrease in pCO_2 was required to account for the magnitude and spatial extent of the late Eocene cooling as well as the EOT itself (*e.g.* DeConto & Pollard, 2003; Elsworth *et al.*, 2017; Goldner *et al.*, 2014; Inglis *et al.*, 2015; Ladant *et al.*, 2014b; Mikolajewicz *et al.*, 1993; Najjar *et al.*, 2002; Sijp *et al.*, 2009). This hypothesis is consistent with pCO_2 reconstructions from various proxies (*e.g.* Anagnostou *et al.*, 2016; Doria *et al.*, 2011; Inglis *et al.*, 2015; Maxbauer *et al.*, 2014; Pagani *et al.*, 2011, 2005; Pearson & Palmer, 2000; Pearson *et al.*, 2009; Tripati *et al.*, 2005). However, despite a moderate effect of DP opening on global temperatures suggested by data and model studies, the actual effects of this gateway opening on changes in ocean structure and dynamics remain to be identified and quantified.

Different geochemical proxies have been used to track water masses and circulation changes through the Eocene, especially oxygen, carbon and neodymium isotopes. Stable isotopes of O and C can reveal changes in environmental characteristics, such as temperature, ice volume and paleoproductivity (*see* Cooke & Rohling, 1999), whereas radiogenic Nd-isotopes can be used to finger-print specific water masses and inter-basin water mass exchange (Frank *et al.*, 2006; Huck *et al.*, 2017; Scher & Martin, 2008; Wright *et al.*, 2018). Based on these proxies, some studies have suggested a priming role for the opening of Eocene gateways on the onset of a modern-like ocean circulation (Borrelli *et al.*, 2014; Katz *et al.*, 2011; Sijp & England, 2004). On the one hand, the DP opening and deepening enabled the formation of the ACC, which connects the Pacific and Atlantic Oceans and encircles Antarctica. This horizontal circulation pattern is particularly visible from changes in Nd-isotope signatures of the South Atlantic, which receives more radiogenic waters originating from the Pacific (Scher & Martin, 2004, 2006). Further, DP opening is often correlated with the contemporaneous onset of a marked difference between Northern and Southern latitude temperatures in the Atlantic Ocean, with cooler temperatures in the high Southern latitudes suggested by $\delta^{18}O$ data (Borrelli *et al.*, 2014; Coxall *et al.*, 2018; Cramer *et al.*, 2009; Katz *et al.*, 2011; Langton *et al.*, 2016). On the other hand, different proxies ($\delta^{13}C$, εNd, $\delta^{18}O$, contourites) suggest the onset of North Atlantic Deep Water formation (NADW) during the late Eocene, which may also have contributed to the thermal differentiation mentioned above (Borrelli *et al.*, 2014;

Coxall *et al.*, 2018; Hohbein *et al*., 2012; Katz *et al.*, 2011; Langton *et al.*, 2016; Scher & Martin, 2008).

Whether these modern-style circulation features suggested by data are reproduced by model studies, and to what intensity, largely varies with model setup and boundary conditions. Notably, the choice of geography (modern or Eocene) and pCO_2 levels plays an important role in explaining the diversity of the results. Furthermore, many studies have focused on surface processes, thus limiting comparison to geochemical proxies.

Several modelling studies have aimed to understand the effect of the DP opening by evaluating its role in modern ocean circulation. These studies use a present-day geography (England *et al.*, 2017; Mikolajewicz *et al.*, 1993; Nong *et al.*, 2000; Sijp & England, 2004, 2005), or an idealized geography such as aquaplanet with idealized continental barriers (Toggweiler & Bjornsson, 2000), and modern pCO_2 levels. These experiments have shown a significant relationship between the opening stage of the DP and the existence and intensity of the ACC and NADW, with a strength of the ACC close to modern observations (between 136.7 ± 6.9 Sv and 173.3 ± 10.7 Sv, Donohue *et al*., 2016; Firing *et al*., 2011; Meredith *et al*., 2011; *e.g.* 140 Sv, Sijp & England, 2004). While a closed DP inhibits the formation of NADW, opening of the DP leads to the onset of deep water formation in the Northern Hemisphere (Mikolajewicz *et al.*, 1993; Nong *et al.*, 2000; Sijp & England, 2005, 2004; Sijp *et al.*, 2009; Toggweiler and Bjornsson, 2000). A decrease in sea surface temperature of as much as 10°C can be produced as a result of these circulation changes (Sijp & England, 2004). Despite the importance of these modeling studies in providing a conceptual understanding of the impact of an open DP on modern oceans, their suitability to represent Eocene ocean changes is questionable. It is expected that studies performed with modern geography and low pCO_2 concentrations reproduce an ocean circulation similar to present day with near-modern ACC, AMOC and NADW intensities. As an intermediate step into Eocene-like boundary conditions, some studies have used higher pCO_2 and/or modified modern geographies with key differences such as an open Panama Seaway (*e.g.* Cristini *et al.*, 2012; Elsworth *et al.*, 2017; Ladant *et al.*, 2018; Sijp & England, 2009; Sijp *et al.*, 2011; Yang *et al.*, 2014; Zhang *et al.*, 2010). The use of an adequate paleogeography is particularly important as it impacts ocean circulation and properties (*e.g.* temperature and salinity distribution, *see* Yang *et al.*, 2014; Zhang *et al.*, 2010). For instance, the closure of the Central American Seaway and the Arctic Ocean, and the subsidence of the Greenland Scotland Ridge have been described as causal mechanisms for NADW onset because of their impact on North Atlantic salinity (*e.g.* Abelson & Erez, 2017; Hutchinson *et al.*, 2018, 2019; Ladant *et al.*, 2018; Mikolajewicz *et al.*, 1993; Sepulchre *et al.*, 2014; Stärz *et al.*, 2017). Experiments with the UVic intermediate complexity model (energy balanced model for atmosphere) and increased pCO_2 alone still describe a strong impact of DP opening on ocean meridional overturning circulation and climate, notably on surface temperatures (Sijp *et al.*, 2009, 2011). Conversely, DP opening in the low-resolution FOAM general circulation model produces a smaller impact in terms of temperature and ocean circulation in an Eocene configuration with high CO_2 levels compared to a modern one (Zhang *et al.*, 2010).

Recent studies have also addressed the question of the DP opening effect on climate using realistic middle Eocene to early Oligocene boundary conditions (Goldner *et al.*, 2014; Hutchinson *et al.*, 2018; Kennedy-Asser *et al.*, 2015, 2019; Vahlenkamp *et al.*, 2018). These studies describe an ACC with a moderate intensity during the Eocene / Oligocene (around 4 Sv to 46.2 Sv, Kennedy-Asser *et al.*, 2015), which strengthens as a result of pCO_2 decrease, Antarctic Ice-Sheet formation and opening of the Southern Ocean (up to 89 Sv, Hill *et al.*, 2013; Kennedy-Asser *et al.*, 2015; Ladant *et al.*, 2014a; Lefebvre *et al.*, 2012; Zhang *et al.*, 2010). Among these studies, the impact of DP opening on temperatures is variable with either a regional cooling of the Atlantic sector of the Southern Ocean (up to 6°C, Kennedy-Asser *et al.*, 2015, 2018) or quasi-insignificant temperature changes (<1°C) (*e.g.* Goldner *et al.*, 2014; Inglis *et al.*, 2015; Zhang *et al.*, 2010). Goldner *et al.*, (2014) have illustrated the particularly weak contribution of the opening of Southern gateways to EOT ocean temperature changes, in comparison to pCO_2 decrease or Antarctic Ice-Sheet build-up. Finally, Northern Hemisphere geography, and especially Arctic geometry, is determinant in the presence or absence of NADW formation, regardless of the configuration of Southern gateways (Hutchinson *et al.*, 2019, 38 Ma paleogeography; Vahlenkamp *et al.*, 2018, 56 - 47.8 Ma paleogeography).

In light of these elements, DP opening is an intermediate stage in the conditions necessary for the onset of modern-like ocean circulation but with a variable, and to some degree model-dependent effect, on ocean temperatures and a high sensitivity to geography. In this paper, we investigate the contribution of DP opening to Eocene ocean changes suggested by geochemical data using the IPSL-CM5A2 Earth System Model (ESM) and realistic Eocene boundary conditions. We perform four simulations with different DP depths (closed, 100, 1000 and 2500 m) and explore the impact of DP opening on the ocean circulation and subsequent temperature changes.

2. Methods

2.1 The model

We use the IPSL-CM5A2 ESM (Sepulchre *et al.* 2019), which is built upon IPSL-CM5A-LR; the CMIP5 ESM developed at IPSL (Institut Pierre-Simon Laplace, Dufresne *et al.*, 2013). As IPSL-CM5A-LR, it is composed of the LMDZ atmospheric model (Hourdin *et al.*, 2013), the ORCHIDEE land surface and vegetation model (Krinner *et al.*, 2005), and the NEMO ocean model (NEMO v3.6, Madec, 2008), which include modules for ocean dynamics (OPA8.2, Madec, 2008), biogeochemistry (PISCES, Aumont *et al.* 2015) and sea-ice (LIM2, Fichefet & Morales-Maqueda, 1997). Atmospheric and oceanic grids are connected via the OASIS coupler (Valcke, 2006). The atmospheric grid has a horizontal resolution of 3.75° longitude $\times$1.875° latitude (96$\times$95 grid points), and is divided into 39 vertical levels. The ocean domain is an irregular tri-polar grid (ORCA2, Madec & Imbard, 1996) with a nominal 2° resolution refined latitudinally up to 0.5° in the tropical region (Dufresne *et al.*, 2013). The ocean is composed of 31 vertical levels whose thickness ranges from 10 m at the surface to 500 m at the bottom. For more detailed descriptions of the model and its different components, the reader is referred to Sepulchre *et al.* (2019).

2.2 Experimental design

2.2.1 Boundary conditions

In order to investigate the role of DP opening on ocean circulation and climate, we perform four simulations with different DP depths (Table 1). These simulations use a 40 Ma paleogeography (Figure 1, see Tardif *et al.*, 2020) and a pCO$_2$ concentration of 1120 ppm (4x Pre-Industrial Atmospheric Levels, PAL) typical of middle Eocene values (Anagnostou *et al.* 2016; Beerling & Royer, 2011). Antarctica is ice-free because prescribed pCO$_2$ levels are above the threshold for perennial polar glaciation in the Eocene (DeConto & Pollard, 2003; Ladant *et al.*, 2014b). Orbital parameters and other boundary conditions are left at their pre-industrial values.

The different Eocene simulations are first compared together to identify the effects of the DP depth on ocean dynamics and properties. Then, as a second step, the simulations are compared to a pre-industrial simulation (CTRL) and another one in which atmospheric pCO$_2$ is increased to 1120 ppm (CTRL-4x). This allows us to have a modern reference frame and to assess the relative importance of both geography and pCO$_2$ on the modern behavior of ocean circulation.

Table 1

Experimental design and volumetric flow rate through the Drake Passage

<table>
<tr><th></th><th>DP depth (m)</th><th>pCO₂ (ppm)</th><th>AIS</th><th>Geography</th><th>DP Flux (Sv)</th><th>Simulation length (year)</th></tr>
<tr><td>DC</td><td>0</td><td rowspan="4">1120</td><td rowspan="4">no</td><td rowspan="4">40 Ma</td><td>/</td><td rowspan="4">4000</td></tr>
<tr><td>D100</td><td>100</td><td>1.3 (sd = 0.2)</td></tr>
<tr><td>D1000</td><td>1000</td><td>21.8 (sd = 1.2)</td></tr>
<tr><td>D2500</td><td>2500</td><td>33.9 (sd = 3.1)</td></tr>
<tr><td>CTRL</td><td rowspan="2">Modern</td><td>280</td><td>yes</td><td rowspan="2">Modern</td><td>109.7 (sd = 8.7)</td><td>2700</td></tr>
<tr><td>CTRL-4x</td><td>1120</td><td>no</td><td>147.3 (sd =11.2)</td><td>3000</td></tr>
</table>

Note. Fluxes were calculated through the Drake Passage (DP), as averages of the last 100 years. They are given in Sverdrups (Sv: 10^6 $m^3.s^{-1}$) and correspond to averages over the last 100 years. Abbreviations: ppm = parts-per-million; sd = standard deviation over the same period (last 100 years).

2.2.2 Model steady state

To what extent the model has reached steady state need to be assessed when analyzing deep ocean circulation (*e.g.* Kennedy-Asser *et al.*, 2018). Our Eocene simulations are run for 4000 years and we use four metrics as indicator of steady state: (1) stability of ocean temperatures at different depths (Figure 2), (2) water conservation through time, (3) stability of the main water masses studied (AABW and ACC, Figure 2, Supporting information Figure S1) and (4) ideal age of ocean waters (Supporting information Figure S2 and S3), which is estimated using 5000 year-long offline age tracer simulations forced by the last 100 years climatology of each fully-coupled simulation. At the end of model integration, temperatures indicate quasi-equilibrium with small trends persisting (< 0.1°C/century) in the deep ocean (Figure 2). This criterion is frequently used as indicative of near equilibrium (*e.g.* Hutchinson *et al.*, 2018; Ladant *et al.*, 2018; Lunt *et al.*, 2017), although the elimination of these trends with further integration would be ideal. The model exhibits only a negligible drift in global salinity (less than 2 cm/century eustatic sea level equivalent change) linked to the not fully conservative LIM2 sea ice model (Sepulchre *et al.*, 2019). In addition, the mean annual intensity of the ACC and the Southern Hemisphere overturning have stabilized by the end of the integration (Figure 2). Finally, the offline age tracer simulations show that the oldest water age in the Pacific, Atlantic and Indian basins is found in the Drake Closed simulation and reaches ~ 2500 years, which suggest that the global overturning of the ocean was completed at least once over the simulation integration time (supporting information Figure S2 and S3). The results shown in this study are averages of the last 100 years.

3. Results

3.1 Changes in ocean dynamics

With a closed Drake Passage (DP), the main upper oceanic circulation patterns of the Southern Ocean can be described as follows (Figure 3). An eastward current, fed by the Brazil and Agulhas currents, exists between South America and Australia. This eastward-flowing current splits into two parts westward of Australia, one branch flows South and the other, to a lesser extent, flows North. Upper ocean waters crossing the Tasmanian Gateway then circulate northward and join the East-Australian Current to finally enter the Ross Gyre or circulate out of the Southern Ocean along the western South America margin. Some South Pacific waters are transferred to the Indian section of the Southern Ocean through the Antarctic Counter Current. As the DP opens, the South Atlantic eastward transport increases, the branch south of Australia strengthens and stops the Antarctic Counter Current, the Ross Gyre weakens and a continuous current (Proto-Antarctic Circumpolar Current) encircles Antarctica. This circulation diminishes inputs of the Brazil and Agulhas currents into the Southern Ocean.

In the 40 Ma experiments (D100, D1000, D2500), horizontal fluxes simulated across the DP are weak (maximum 33.9 Sv) but show some substantial changes owing to deepening of the DP. A maximum difference of 32.6 Sv is observed between D100 and D2500. Simulations with a modern geography exhibit a stronger ACC, comparable to published estimations (between 136.7 ± 6.9 Sv and 173.3 ± 10.7 Sv, Donohue *et al.*, 2016; Firing *et al.*, 2011; Meredith *et al.*, 2011). The transport through the DP is larger in CTRL-4X than in CTRL. This result suggests a positive impact of pCO_2 on ACC strength with a modern geography. The different mechanisms driving this westward circulation will be introduced and their respective roles discussed in section 4.2.

At 40 Ma, all deep convection takes place in the Southern hemisphere whereas mixed-layer depths (MLD) in the Northern Hemisphere do not exceed 500 m (Figure 4). When the DP is closed, sinking occurs in the Atlantic sector of the Southern Ocean and to a lesser extent in the Indian sector (Figure 4). DP opening reduces the depth of these convection zones. Deep convection persists in a small area of the Weddell Sea, but completely ceases in the Indian sector of the Southern Ocean (Figure 4). In contrast, new deep convection areas develop in the Pacific sector of the Southern Ocean.

With a closed DP, the meridional overturning circulation is essentially restricted to intermediate waters (< 1500 m depth) in the Atlantic Basin (Figure 5). Despite significant deep sinking in the Weddell Sea, meridional water transport is weak. When the DP opens, as deep convection shifts to the wider and deeper Pacific Ocean basin, a larger and more intense Southern Hemisphere overturning cell forms and expands northward up to 40°N. These changes in convection zones and meridional transport occur even for shallow DP depths (D100). As the DP deepens (D100 to D2500), flow of Antarctic Intermediate Waters (AAIW; here defined as the maximum of the absolute overturning of the Southern hemisphere < 1500 m deep waters) diminishes; Antarctic Bottom Waters (AABW; here defined as the maximum of the absolute overturning of the Southern hemisphere > 1500 m deep waters) sink deeper and overall maximum overturning is reduced. In all the Eocene experiments, the Southern Hemisphere drives the meridional overturning circulation. There is no source of deep or intermediate waters in the Northern Hemisphere (Figure 4 and 5, supporting information Figure S4). More freshwater is routed to the high-latitudes (poleward of 50°) in the Northern Hemisphere than in the Southern Hemisphere regardless of the configuration of the Drake Passage. The North Atlantic basin receives ~ 42% more freshwater than the South Atlantic and the North Pacific basin receives ~ 36% more freshwater than the South Pacific (supporting information Table S1). These larger freshwater fluxes in the northern high-latitudes are primarily related to larger runoff inputs in the northern basins (supporting Table S1) and participate to the freshening of surface waters, increasing their buoyancy.

3.2 Change in ocean properties and Antarctica climate

In addition to the ocean circulation changes described above, DP opening also affects ocean properties. With a closed DP, the mean annual global Sea Surface Temperature (SST) is 28.6°C. The opening of the DP has little effect on mean annual global SST even with a 2500 m depth (< 0.5°C; Figure 6, Table 2). However, at a regional scale (40°S-80°S), the opening of DP results in significant changes, which differ from one basin to another. SSTs decrease similarly in the Atlantic and Indian sectors of the Southern Ocean when the DP is open to 100 m (1.2°C in each basin; Table 2). But the effect of DP opening on Southern Ocean temperatures is not linear. Opening from 100 to 1000 m indeed produces more of a cooling effect (1.7°C in average across the Southern Ocean, locally up to 5.8°C in the Kerguelen Plateau area) than opening from 1000 to 2500 m (in fact, the Southern Ocean even warms slightly on average, Table 2). In contrast, the Pacific sector of the Southern Ocean exhibits a large warming zone surrounded by cooling areas (Figure 6), but there is no clear tendency for warming or cooling with DP deepening (Table 2). The SST reconstructed with our simulations are in a moderate agreement with proxy-data reconstructions for the late-middle Eocene (Figure 7; data compilation from Tardif *et al*., 2020, modified after Baatsen *et al*., 2020). Although most estimates are within our confidence interval, which represents the longitudinal range of annual temperatures, there is a tendency to underestimate high latitude temperatures and overestimate low latitude temperatures for all the simulations. Because it results on average in a cooling of the Southern Ocean (Table 2), the opening of the Drake Passage tends to strengthen the latitudinal temperature gradient in the Southern Hemisphere (Figure 7). Changes in surface temperature effect is well explained by changes in Southern Ocean deep convection changes and their evolution on both sides of the DP as the DP deepens. On the one hand, deep water sinking in the Pacific Southern Ocean tends to attract lower-latitude warm surface waters toward the Southern Ocean. On the other hand, the decline of Weddell Sea and South Indian convection induces a decrease in heat transfer toward this other sector of the Southern Ocean. After the main convection zone shifts from the Atlantic to the Pacific sector, the Weddell convection is suppressed, whereas Ross Sea convection only slightly weakens (Figure 4). A slight increase in sea surface salinity is observed through most of the ocean with DP deepening. In the Southern Ocean salinity changes follow the same trends as sea-surface temperatures (*i.e.* an increase in the Pacific sector of the Southern Ocean and a decrease in the Atlantic sector of the Southern Ocean, see supporting information Figure S5).

Table 2

Sea surface and 2 m atmospheric temperatures

	Sea surface temperatures					2 m atmospheric temperatures			
	SST	SO	PSO	ASO	ISO	SAT	Ant.	Ant. JAS	Ant. JFM
DC	28.6	18.1	17.3	17.4	20.4	26.7	6.0	-6.7	21.3
D100	28.3	17.7	17.5	16.3	19.2	26.4	4.6	-8.2	20.3
D1000	28.1	16.5	16.9	14.9	17.0	26.3	3.7	-8.9	19.1
D2500	28.1	17.0	17.4	15.6	17.4	26.2	3.7	-9.6	19.8

Note. Mean annual surface temperatures (°C) are given as global mean (SST) or averaged over the Southern Ocean (40°S - 80°S, SO) and its different sectors: Pacific (PSO), Atlantic

(ASO) and Indian (ISO). Atmospheric 2m temperatures (°C) are given as annual mean averaged globally (SAT) or over Antarctica (Ant.). Ant. JAS and JFM represent the austral winter and summer mean respectively.

In the DC experiment, global Ocean Heat Transport (OHT) is asymmetric with stronger transport toward the Southern than toward the Northern Hemisphere (Figure 8; on average ~ 30 % higher than in modern experiments 10°S - 65°S). Opening the Drake Passage shifts the OHT towards a modern state and induces a net southward OHT decrease (13.4%) between 10°S - 60°S.

DP opening and the formation of a proto-ACC also affect Antarctic continental climate. Our simulations exhibit a 1 to 4°C cooling in the 2-meter air temperatures with largest values occurring over the Atlantic sector of continental Antarctica (Table 2 and Figure 9), even though the largest absolute change occurs over the Indian sector of the Southern Ocean. In conjunction with the changes in deep-water formation areas, changes in low cloud cover contribute to cooling the Indian sector of the Southern Ocean by increasing planetary albedo (Figure 9). The existence of two low-pressure cells located over deep-water formation areas in the modern Weddell and Ross Seas in D2500 (Figure 9) and a higher-pressure cell in the Indian sector of Antarctica leads to poleward flow of Atlantic-Indian air masses, carrying the Indian cooling signal to Antarctica. This atmospheric reorganization explains why the Antarctic continent cools rather than warms, even if the Southern Ocean exhibits both cooling and warming zones.

The simulated Antarctic cooling in our simulations is comparable to that of Kennedy-Asser *et al.* (2019), who simulate a cooling of 3°C in Antarctica for comparable boundary conditions. This result is also consistent with studies suggesting that the opening of the Drake Passage may have contributed to create favorable climatic conditions for the onset of the Antarctic Ice Sheet but was likely not the main direct catalyst of this event (DeConto & Pollard, 2003; Ladant *et al.*, 2014b).

Opening the DP leads to the cooling of most deep ocean waters (here defined as waters below 1500 m; Figure 10). The Atlantic, Indian and Pacific Ocean temperatures drop by as much as 2.5°C in some areas. These temperature changes are rather constant across latitudes for any given depth in the Pacific and Indian Oceans, but the cooling is stronger at southern mid- to high latitudes in the Atlantic basin. The cooling of deep waters is accompanied by warming of intermediate waters (*i.e.* between 300 m and 1500 m) in all basins (locally as much as 4.5°C). This warming extends from the basins' northernmost latitudes down to 40°S for the Atlantic and Indian Ocean and 60°S for the Pacific Ocean. This pattern is consistent with the deepening of the meridional stream function, which is the result of the initiation of deep-water production in the South Pacific, and reduction in deep-water formation in the South Atlantic when the DP opens. The existence of a MOC in the wide and deep Pacific basin, in addition to the diminished Atlantic MOC, reduces the imprint of the Atlantic MOC on overall ocean circulation and physical properties, leading to a warming of North Atlantic intermediate and deep waters and a cooling of Pacific and Indian deep waters (Figure 5). These vertical cooling and warming patterns are observed in all DP opening experiments (D100 to D2500). Cooling or warming intensity depends on gateway depth but does not vary linearly, with the strongest differences occurring in D1000, as is also the case for surface temperatures (supporting information Figure S6).

Following the water temperature and salinity changes mentioned above, potential water density and pressure gradients increase in the Southern Ocean (Figure 11). In the latitudinal band of 65°S to 45°S, the pressure gradient increases from 0.5 kg/m^3 in DC to 0.6 kg/m^3 in D2500 and to 0.9 kg/m^3 in CTRL-4X at 400 m depth; and from 0.2 kg/m^3 in DC and D2500 to 0.5 kg/m^3 in CTRL-4X at 800 m depth.

In order to better understand the behavior of the proto-ACC, Southern hemisphere horizontal surface wind changes were also tracked (Figure 11). Indeed, horizontal surface winds are often given a key role in explaining ACC strength, notably, the westerlies that directly blow on this current (Scher *et al.*, 2015). Compared to modern simulations, Eocene experiments have weaker winds and a more equable distribution across latitudes. Because of steeper temperature gradient and the presence of the Antarctic ice sheet, CTRL shows stronger polar easterlies (South of the DP) and the maximum intensity zone of the westerlies is located ~ 5° further North. A few differences are observed as the DP depth is increased. The westerlies (~ 50°S - 30°S) and polar easterlies (South of the DP) are slightly strengthened, with a maximum difference of 0.6 $m.s^{-1}$ and 1.1 $m.s^{-1}$ respectively (D2500 *minus* DC).

Discussion

4.1 Results Summary

Opening the Drake Passage (DP) impacts Southern Hemisphere ocean dynamics and properties in several ways. First, it leads to the formation of a continuous proto-ACC, which leads to a modification of surface temperatures and salinities patterns across the Southern Ocean. Second, an open DP favors deep-convection in the Pacific sector of the Southern

Ocean instead of the Atlantic and Indian sectors. Third, it strengthens the meridional overturning circulation. Fourth, it induces cooling of most of Pacific and Indian Ocean deep waters, but induces an asymmetric cooling in the Atlantic Ocean, in which only South Atlantic deep waters cool whereas North Atlantic deep waters warm. Some of these changes may characterize the transition from an Eocene to a modern ocean.

In the following section, we discuss the implications of our results for the evolution of ocean properties and dynamics described by proxy data and compare our results with previous modeling work. We focus in particular on the onset of the ACC, on South Atlantic cooling and on the initiation of NADW. It is worth noting that some previous studies have focused on the role of other potential controls on the Eocene ocean circulation, such as the opening of the Tasmanian Gateway or the development of the Antarctic Ice Sheet (*e.g.* Goldner *et al.*, 2014; Huber *et al.*, 2003, 2004, Kennedy-Asser *et al.*, 2015, 2019), but, as these controls remain constant in our experiments, we mainly discuss our results with respect to previous work focusing on the oceanic impact of changes in DP depth.

4.2 Proto-ACC onset

4.2.1 Formation of the proto-ACC

Our results are consistent with inferences from proxy-based data studies that describe a complete but moderate proto-ACC during the late Eocene (Borrelli *et al.*, 2014; Scher & Martin, 2004, 2006). In our closed DP experiment, circulation through the TG consists of an eastward branch from the Atlantic in the North of the passage and a westward branch (the Antarctic Counter Current) flowing along the margins of Antarctica. When the DP is open, the eastward transport through the TG strengthens and the Antarctic Counter Current ceases to exist (Figure 3). This circulation pattern is in agreement with former studies showing a westward exchange during the middle Eocene (Bijl *et al*., 2013; Huber *et al*., 2004; Sijp *et al*., 2016) and its cessation with DP opening (Sijp *et al*., 2016).

Multiple terms exist to qualify the earliest stages of the ACC. Borrelli *et al.* (2014) make the distinction between a "Drake Throughflow" and a "proto-ACC" depending on the current trajectory and depth around Antarctica. The "proto-ACC" encircles Antarctica but is shallower than the modern ACC. In our Eocene simulations, water transports of 1.3 to 33.9 Sv through the DP are by far weaker than the modern ACC (observed: 136.7 ± 6.9 Sv and 173.3 ± 10.7 Sv, Donohue *et al*., 2016; Firing *et al.*, 2011; Meredith *et al*., 2011, or simulated: 108.9 Sv in CTRL). Nevertheless, this weak eastward current exists around Antarctica in our open DP simulations even for shallow DP depths, consistent with the concept of a proto-ACC. A proto-ACC circulation is supported by changes in the εNd signatures of the South Atlantic and South Indian Oceans by 37 - 41 Ma (Pfister *et al*., 2014; Scher & Martin, 2006, 2004; Wright *et al.*, 2018). Furthermore, other evidence from εNd and $\delta^{13}C$ isotopes suggest the initiation of a modern-like ACC later, between the early Oligocene (Katz *et al.*, 2011; Scher *et al.*, 2015), late Oligocene (Borrelli *et al.*, 2014) and the Oligocene-Miocene boundary (Scher & Martin, 2008). The simulated transport intensities across the DP in our Eocene simulations are also within the range of previous model studies using similar Eocene boundary conditions with reported values ranging from 4 Sv to 46.2 Sv (Hutchinson *et al*., 2018; Kennedy-Asser *et al*., 2015; Ladant *et al*., 2014a; Zhang *et al*., 2010). Together, our results agree with former comparable modelling studies and geochemical records to indicate that a proto-ACC formed before the EOT, as soon as the DP started to open.

4.2.2 Driving factors of proto-ACC intensity

The difference in ACC intensity between our Eocene scenarios and the two simulations with a modern geography suggests a significant sensitivity to changes in geography. The DP is located in the Scotia arc, a complex tectonic region in which the Scotia Plate, the Antarctic Plate, and the South American plate interact together through a set of subductions zones and transform faults (Barker *et al*., 2001; Dalziel *et al*., 2013; Eagles & Scott, 2014). Related to the development of the scotia plate, DP opening would have taken place gradually, starting about 50 Ma ago (Eagles *et al*., 2006; Livermore *et al*., 2005). The first evidence of seafloor spreading indicates the formation of a shallow (< 1 km) connection between Pacific and Atlantic oceans around 41 Ma but such passage was probably narrow and tortuous before 30 Ma (Eagles & Jokat, 2014). The presence of a continuous wide and deep passage (100-300 km width, > 2.5 km depth) is documented around 26-20 Ma (Eagles & Jokat, 2014). However, the past position of the blocks that form this region and its paleogeography remains poorly constrained (Barker *et al*., 2001; Eagles, 2010; Galindo-Zaldívar *et al*., 2014), hampering direct comparison with data (Sijp *et al*., 2014). Nd-isotope signatures from the Kerguelen Plateau and locations around the Antarctic continent do not suggest major oceanographic changes related to DP opening before 44 Ma (Huck *et al*., 2017) or after ~36 Ma (Wright *et al*., 2018), suggesting that sufficient opening of the DP to allow water mass mixing took place in the middle Eocene (Wright *et al*., 2018). Nd-isotope data from two locations in the Atlantic sector of the Southern Ocean, OPD Sites 1090 and 689, exhibit a positive shift between 42 to 39 Ma, superimposed on an increasing trend, suggesting an influx of shallow Pacific waters carrying a more radiogenic Nd-isotope signature (Scher and Martin, 2004; 2006). Finally, a middle Eocene surface opening of the Drake Passage is supported by multi-variate analyses of dinoflagellate cyst occurrences at sites in the Drake Passage area (Estebenet *et al*., 2014).

Besides the degree of opening of the DP, the depth of the Tasmanian Gateway and the Kerguelen Plateau might limit the proto-ACC strength (Hill *et al*., 2013; Scher *et al*., 2015). The Kerguelen Plateau formation is related to volcanic activity. It started in the Cretaceous for its southern and central parts and ~ 40 Ma for its northern part (Wright *et al*., 2018). During the Eocene, most of the northern parts of the plateau were submarine (~ 870 m) and the southern part reached between ~1200 – 2250m below sea level (Wright *et al*., 2018). In our paleogeographic reconstruction (40 Ma, see Tardif *et al*., 2020), the Kerguelen Plateau is shallower than at the present day (mostly 1000 to 1500 m depth, locally up to 400 m) and the Australian and Antarctic continents are closer. Our reconstructed depth for the Tasmanian Gateway varies between 500 m to 600 m near the continental margins, and between 1000 m to 2500 m, in its central part, which may favor water exchange, although flow remains very low compared to modern. Studies based on dinocyst distribution patterns suggest an initial TG opening during the early Eocene ~49-50 Ma (Bijl *et al*., 2013) followed by accelerated deepening in the late Eocene (~35.7 Ma; Houben *et al*., 2019). The latter deepening is consistent with widespread occurrence of unconformities in the Australian-Antarctic basin through non-deposition or erosion, indicative of bottom current intensification (Sauermilch *et al*., 2019). Rather than a later date for TG deepening between 35.5 Ma and 33.7 Ma (Carter *et al*., 2004; Exon *et al*., 2004; Stickley *et al*., 2004), changes in temperature (Cramwinckel *et al*., 2018) and pCO_2 (Anagnostou *et al*., 2016), and/or northward movement of the Tasmanian region (Scher *et al*., 2015), may explain oceanographic changes near the EOT (Houben *et al*., 2019).

In addition to the depth of sub-oceanic structures, it has been proposed that the latitudinal distribution of land barriers and gateways was critical in determining ACC strength (*e.g.* Hill *et al*., 2013; Scher *et al*., 2015; Stickley *et al*., 2004). The importance of latitudinal structures has been called into question because the modern ACC meanders between the latitudes of the DP and the latitudes of maximum wind stress (Allison *et al*., 2010; Rintoul *et al*. 2001), such as in the Malvinas Current region to the east of Argentina. Interestingly, our open DP simulations exhibit a similar current system that meanders across latitudes (Figure 3).

Although the depth and width of the DP may be the dominant control on differences in water transport through the DP between simulations (*e.g.* Kennedy-Asser *et al*., 2015; Sijp &

England, 2004; Yang *et al*., 2014; Zhang *et al*., 2010), other parameters may contribute to ACC intensity, in particular the meridional density gradient and wind stress (Gent *et al*., 2001; Lefebvre *et al.*, 2012; Marshall *et al*., 2016). Using an eddy-permitting ocean model in an idealized channel configuration, Munday *et al.* (2015) suggest that the absence of overlapping continental barriers is not a necessary condition for strong circumpolar transport. However, the number of continental barriers, their latitudinal location, and whether they are overlapping may act on ACC strength by impacting its sensitivity to wind stress (Munday *et al.*, 2015). In our simulations, the majority of wind strength changes between D2500, CTRL and CTRL-4X takes place within the maximum eastward wind zone where a portion of the proto-ACC flows (Fig. 9). This variable sensitivity of the ACC to wind stress might exist in our results but would need additional sensitivity experiments.

In parallel, proto-ACC strength correlates with meridional density gradients in our simulations, where the strongest water transport (*i.e.* D2500, CTRL, CTRL-4X) corresponds to the steepest isopycnals (Figure 11). The link between the intensity of the ACC and meridional density gradients has been reported by previous modeling studies (Goldner *et al.*, 2014; Kennedy-Asser *et al.*, 2019, 2015; Ladant *et al.*, 2014a; Lefebvre *et al.*, 2012). Additionally, the latitude of the Southern Hemisphere westerlies (~ 50°S - 30°S) is slightly displaced to the South, closer to modern ACC flow, which might also contribute to reinforcing the horizontal transport in this simulation (Figure 11).

4.3 Changes in ocean properties and dynamics, and N/S thermal differentiation

4.3.1 Surface temperature changes

In our experiments, the opening of the DP impacts surface and deep-water temperatures in all basins. Most surface changes occur in the Southern Ocean, which exhibits a dipole pattern, with cooling in the Atlantic and Indian sectors and a warming zone in the Pacific (Figure 6). The presence of a warming zone in part of the Southern Ocean (here in the Pacific) has already been described in previous modeling studies with modern as well as Eocene paleogeographies (Cristini *et al.*, 2012; Sijp & England, 2004; Zhang *et al.*, 2010). It is well explained by changes in the distribution of deep convection zones that impact the southward inflow of warm subtropical waters (Kennedy-Asser *et al.*, 2015; Ladant *et al.*, 2018) and by the weakening of the Brazil and Agulhas currents (as seen by Sijp & England, 2004). Our simulated temperature changes with cooling in the Atlantic and Indian sectors and warming in the Pacific are similar to those described in previous model studies (Cristini *et al*., 2012; Zhang *et al*., 2010). In contrast to this dipole pattern, a more homogenous and up to 4°C surface atmospheric cooling has been described over southernmost latitudes (Yang *et al.*, 2014).

Our results are in a moderate agreement with proxy-data SST reconstruction. On the one hand, our model tends to overestimate the latitudinal temperature gradient and to reconstruct colder temperatures than some proxies in the Southern Ocean (Figure 7). This bias is very classical in warm climate reconstructions with GCMs, and could be responsible for a discrepancy between absolute SST from our experiments and proxies (see Huber & Caballero, 2011). Studies carried out with more recent versions of GCM, such as CESM and GFDL, show improvements in the representation of this gradient, in particular thanks to a better consideration of cloud physics and other greenhouse gases (Baatsen *et al.*, 2020; Hutchinson *et al.*, 2020; Lunt *et al.*, 2020; Sagoo *et al.*, 2013; Zhu *et al.*, 2019). With close boundary conditions, they reconstruct flatter gradients thanks to ~ 3°C lower SST in equatorial area and up to 2°C to 3°C higher SST at mid-latitudes (supporting information Figure S7; Baatsen *et al.*, 2020; Hutchinson *et al.*, 2018). Opening the DP tends to reinforce the latitudinal temperature gradient by mainly cooling Southern latitudes. It therefore does not create a better agreement with the absolute surface temperature data for this period. This trend suggests that the DP opening and the implementation of a proto-ACC may have contributed to the establishment of the modern gradient. On the other hand, multi-proxy data indicate warmer SSTs in the Pacific Southern Ocean than in the Atlantic during the middle and late Eocene (Douglas *et al.*, 2014; Hollis *et al.*, 2012; Liu *et al.*, 2009), which is well explained by convection in the Ross Sea and coherent with εNd reconstructions indicating the northward export of Southern Ocean Deep water between 45 and 35 Ma (Douglas *et al.*, 2014; Hague *et al.*, 2012; Thomas, 2004; Thomas *et al.*, 2014). Interestingly, this is not incompatible with locally intensive cooling described near the Tasman Plateau (Bijl *et al.*, 2009; Hollis *et al.*, 2012), since our simulated SST changes in the Pacific sector of the Southern Ocean are heterogeneous with cooling areas (around Antarctica).

In studies with modern or near-modern geographies, significant warming in the Northern Hemisphere, locally up to 6-12°C, is also observed (Elsworth *et al.*, 2017; Sijp & England, 2004; Toggweiler & Bjornsson, 2000; Yang *et al.*, 2014). This warming at northern latitudes is explained by changes in the meridional overturning circulation, mainly with the onset of North Atlantic Deep Water formation (NADW), and a subsequent increase of northward Oceanic Heat Transport (OHT; Elsworth *et al.*, 2017; Sijp & England, 2004; Toggweiler & Bjornsson, 2000; Yang *et al.*, 2014; Zhang *et al.*, 2010). Therefore, the absence of such a warming in the Northern Hemisphere might be explained by the lack of NADW formation in our experiments. This absence of NADW is discussed in more detail in section 4.4.

4.3.2 Intermediate / deep ocean changes

Our results show a significant impact of the opening of the DP on deep ocean temperatures, which decrease in every basin except the North Atlantic by an amount consistent with earlier modeling work (Najjar *et al.*, 2002; Nong *et al.*, 2000; Sijp *et al.*, 2009). The latitudinal extent of temperature changes is intimately linked to the strength of the meridional circulation (*e.g.* Goldner *et al.*, 2014; Najjar *et al.*, 2002; Sijp *et al.*, 2011). Here, the northward propagation of cooling in the Pacific Ocean is due to deep convection in the Ross Sea when the DP is open, which shifts the core of the MOC in the Pacific. Conversely, more regional changes in the Atlantic are linked to the weakening of deep convection in the Weddell Sea. Finally, as no deep-water forms in the Indian Ocean in either an open or a closed DP configuration, the cooling trend observed in the Indian Ocean basin comes from transport of cold deep waters from the Pacific (supporting information Figure S8). Our results contrast with the findings of Goldner *et al.* (2014) who show a minor contribution of Southern gateway changes to the Atlantic Ocean cooling (because of the opposite effects of DP deepening and Tasman Gateway opening on temperatures), using a configuration with a closed Tasmanian Gateway, which likely explains the significant differences between our studies. Furthermore, in contrast to our Eocene experiments with an open DP, the simulations of Goldner *et al*. (2014) do not produce a strong overturning circulation, which might limit the effect of any regional temperature change in the Southern Ocean.

Among studies using Eocene geographies, some find similar results with a shift in deep convection zones and AABW strengthening in response to Antarctic Ice Sheet building (Goldner *et al.*, 2014; Kennedy-Asser *et al.*, 2015, 2019). However, model gateway opening experiments yield different results concerning the stability of deep convection in the Weddell Sea and show that the response might be model dependent and / or rely on paleogeographic differences, notably in the North Atlantic - Arctic area (Hutchinson *et al.*, 2019; Vahlenkamp *et al.*, 2018).

The deep temperature changes observed among the different basins are in agreement with geochemical proxy reconstructions. In the Atlantic Ocean, several studies have documented thermal differentiation between the North and South Atlantic with a ~ 2°C cooling of southern high latitudes, represented by a ~ 0.5‰ $\delta^{18}O_{bf}$ difference, starting between 38.5 Ma and 35 Ma (Borrelli *et al.*, 2014; Coxall *et al.*, 2018; Cramer *et al.*, 2009; Katz *et al.*, 2011; Langton *et al.*, 2016; Liu *et al*., 2018). Southern Hemisphere cooling in the Atlantic basin has often been interpreted as an indicator of the onset of a proto-ACC and of a decreased southward OHT (Borrelli *et al.*, 2014; Katz *et al*., 2011; Langton *et al.*, 2016). Borrelli *et al*. (2014) further describe brief warming of North Atlantic deep waters occurring contemporaneously to the thermal differentiation (~ 38.5 Ma), and interpret this warming as the signature of deep-water formation in the Northern Hemisphere. As an alternative to this mechanism, we show that the opening of the DP also limited northward cold-water export into the Atlantic.

The cooling of the deep Indian Ocean by inflow of Pacific waters is consistent with studies that describe an increase of the εNd signature in the Indian Ocean basin and on the Kerguelen Plateau during the middle and late Eocene (Huck *et al*., 2017; Le Houedec *et al*., 2012; Martin & Scher, 2006; Scher & Martin, 2004; 2006; Scher *et al*., 2011), which may be explained by an increased inflow of waters originating from the Pacific, which generally carry a higher εNd signature (Van de Flierdt *et al*., 2004; Hague *et al*., 2012; Le Houedec *et al*., 2016; Scher *et al*., 2015; Thomas *et al*., 2014). These Pacific waters may either originate from the onset of the ACC or the Indonesian Throughflow (Frank *et al*., 2006; Martin & Scher, 2006). Interestingly, our simulations indicate a shift in deep-water transport to the Indian Ocean. In a closed DP configuration, deep waters from the Atlantic sector of the Southern Ocean flow through the Indian Ocean toward the Pacific Ocean, whereas in a DP open configuration, the Indian Ocean is filled by deep waters flowing westward from the Pacific Ocean through the Indonesian Throughflow (supporting information Figure S8).

Finally, the simulated deep Pacific Ocean cooling not easily reconciled with geochemical data. Eocene deep ocean temperature reconstructions are scarce for this basin (one equatorial site, ODP 1218) and do not indicate a decrease in deep ocean temperatures during the late Eocene (Borrelli *et al*., 2014).

4.4 Circulation changes and the absence of NADW

Along with the observed N/S thermal differentiation may have come the initiation of NADW formation during the Eocene. The existence of Northern Component Water potentially as early as 38.5 Ma is suggested by changes in North Atlantic $\delta^{13}C$ signature of benthic foraminifera at ODP Site 1053 (Borrelli *et al*., 2014). The authors interpret the high $\delta^{13}C$ signal at this bathyal site as evidence for sinking waters in the North Atlantic. Further, the intensification of southward transport by 35 Ma is suggested by the decreasing horizontal $\delta^{18}O$ gradient between the North and Equatorial Atlantic (Langton *et al*., 2016; site 1053 and site 366). In contrast, the multi-site study by Coxall *et al*. (2018) indicates a slightly later onset of Northern Component Water (~ 35.8 - 33.8 Ma) because the reduced difference in $\delta^{18}O$ signatures of benthic and planktonic foraminifera suggests a decrease in water column stratification and a better convection of the North Atlantic during this period. A change in the ε_{Nd} signatures of South Atlantic and Southern Ocean Sites between the late Eocene and the late Oligocene has been interpreted as increased southward advection of North Atlantic deep water (Scher & Martin, 2008; Via and Thomas, 2006; Wright *et al.*, 2018). Possible contourites may also suggest the existence of NADW during the Eocene (Hohbein *et al*., 2012), although this is debated (Stocker *et al*., 2013).

Previous model studies using modern geography indicate the onset of NADW formation following DP opening (Mikolajewicz *et al.*, 1993; Nong *et al.*, 2000; Sijp & England, 2005, 2004; Sijp *et al.*, 2009; Toggweiler & Bjornsson, 2000; Yang *et al.*, 2014). Several geographic changes might, however, be necessary to simulate the onset of NADW formation, notably the closure of the Panama Seaway and the closure of the Arctic-Atlantic gateway (Bice *et al*., 2000; Hutchinson *et al*., 2018, 2019; Roberts *et al*., 2009; Vahlenkamp *et al*., 2018; Yang *et al*., 2014). As discussed in details by Ladant *et al.* (2018), there is significant variability in NADW reconstruction among model studies, and the geometry and depth of the Panama Seaway are likely instrumental in the existence of NADW in models using a modern geography (Ladant *et al.*, 2018; Mikolajewicz *et al.*, 1993; Sepulchre *et al.*, 2014; Zhang *et al*., 2012). In some studies, the Panama Seaway allows for extensive freshwater transport from the Pacific to the North Atlantic, which decreases North Atlantic seawater and may limit the onset of NADW formation (Ladant *et al.*, 2018; Sepulchre *et al.*, 2014; Yang *et al.*, 2014; Zhang *et al*., 2012). In our simulations, surface waters from the Mediterranean Sea flow across the North Atlantic and through the Panama Seaway. This process forms a salt leak in the Pacific Ocean that limits water density in the North Atlantic and may be responsible for the absence of NADW formation.

In experiments with an Eocene paleogeography, the connection between the Arctic Ocean and the North Atlantic has been described as a controlling factor in the onset of NADW formation (Hutchinson *et al*., 2018, 2019; Roberts *et al*., 2009; Vahlenkamp *et al*., 2018). In these experiments, a connection between both basins hampers deep convection in the North Atlantic because of Arctic freshwater inputs. Apparent variability of salinity and ventilation of the Arctic Ocean during the Eocene supports changes in the Arctic and Atlantic connection during Eocene (Brinkhuis *et al*., 2006; Jakobsson *et al*., 2007). Alternatively, a number of studies have suggested that subsidence of the Greenland-Scotland Ridge (GSR) at ~36 Ma was a prerequisite for NADW formation (*e.g.* Abelson & Erez, 2017; Borrelli *et al*., 2014; Coxall *et al*., 2018; Hutchinson *et al.*, 2018; Katz *et al*., 2011; Stärz *et al*., 2017). In this hypothesis, deep water forms in the Nordic Seas during the Eocene but the Greenland-Scotland Ridge blocks its southward export (Abelson & Erez, 2017; Abelson *et al*., 2008). In our paleogeography, this ridge is sufficiently subsided but no deep convection occurs in the Northern Hemisphere. Oceanic barriers further south, including the Equatorial Atlantic Gateway and the Rio Grande Rise-Walvis Ridge barrier, had sufficiently subsided to allow the exchange of deep water between the Atlantic basins and the Southern Ocean before the Eocene (Batenburg *et al*., 2018; Pérez-Díaz & Eagles, 2017). Therefore, our results do not support a blocking of NADW export but rather suggest that the absence of NADW formation depends on surface water properties.

The existence of NADW has also been linked to the intensity of the ACC (Langton *et al*., 2016; Scher & Martin, 2008). Theoretical modelling experiments have shown a relationship between modern ACC and NADW intensities. This so-called "Drake Passage effect" hypothesis (Toggweiler & Samuels, 1995; *see* Kuhlbrodt *et al*., 2007 for a review) is based on a conceptual model in which the MOC and NADW formation are driven by Southern Ocean wind-driven upwelling, generated by the presence of the ACC. However, the potential covariability of the ACC and the MOC is probably highly dependent on geography and remains to be demonstrated with realistic paleoclimate modelling experiments.

Finally, it is worth noting that previous studies based on modeling (Hutchinson *et al*., 2018; Thomas *et al*., 2014) and Nd isotope measurements (Hague *et al*., 2012; McKinley *et al*., 2019; Thomas *et al*., 2014) have suggested the formation of deep-water in the North Pacific during Late Cretaceous/Paleogene. However, the existence of North Pacific Deep Water in the Late Cretaceous/Paleogene Ocean is still debated. Indeed, North Pacific sinking is absent from several recent Eocene earth system model simulations (Baatsen *et al*., 2020; Farnsworth et al. 2019; Kennedy-Asser *et al*., 2015; Lunt *et al*., 2016; Vahlenkamp *et al*., 2018). Additionally, recent ε_{Nd} samples from the tropical and equatorial Pacific Ocean argue against the possibility of deep-water formation in the North Pacific until at least the latest Cretaceous (Haynes *et al*., 2020). Our simulations exhibit significant runoff freshwater fluxes in this basin, which freshen North Pacific surface waters and render them more buoyant, hampering deep convection in this area.

Conclusion

Our simulations of the effect of the opening of the Drake Passage on ocean circulation patterns and paleo-environmental conditions are in a rather good agreement with proxy data. We show that DP opening has a strong effect on Southern Ocean physical properties and dynamics from a depth of 100 m onwards. It sets the stage for the formation of a proto-ACC and initiates changes in deep convection zones and in the meridional overturning circulation. Most deep waters experience cooling, which is characterized by an asymmetric distribution in the Atlantic Ocean. This pattern is in particularly good agreement with proxy-based reconstructions, which indicate a North/South thermal differentiation in this basin since 38.5 to 37.5 Ma. Therefore, our simulations robustly describe how the Eocene opening of the DP constitutes an important step towards the onset of a global thermohaline circulation similar to the present day.

4. Acknowledgments, Samples and Data

We thank the CEA/CCRT for providing access to the HPC resources of TGCC under the allocation 2017-A0010102212, 2018-A0030102212 and 2019-A0050102212 made by GENCI. We acknowledge the support of the ERC MAGIC under the grant 649081. The authors acknowledge Michiel Baatsen for sharing is data outputs from the CESM model. We acknowledge use of Ferret (ferret.pmel.noaa.gov/Ferret/) and NCL software for analysis and figures in this paper. The key climatological outputs of the simulations are stored in the PANGAEA database (https://doi.pangaea.de/10.1594/PANGAEA.915802).

5. References

Abelson, M., Agnon, A., & Almogi-Labin, A. (2008). Indications for control of the Iceland plume on the Eocene–Oligocene “greenhouse–icehouse” climate transition. *Earth and Planetary Science Letters*, *265*(1–2), 33–48. https://doi.org/10.1016/j.epsl.2007.09.021

Abelson, M., & Erez, J. (2017). The onset of modern-like Atlantic meridional overturning circulation at the Eocene-Oligocene transition: Evidence, causes, and possible implications for global cooling. *Geochemistry, Geophysics, Geosystems*, *18*(6), 2177–2199. https://doi.org/10.1002/2017GC006826

Allison, L. C., Johnson, H. L., Marshall, D. P., & Munday, D. R. (2010). Where do winds drive the Antarctic Circumpolar Current? *Geophysical Research Letters*, *37*(12). https://doi.org/10.1029/2010GL043355

Anagnostou, E., John, E. H., Edgar, K. M., Foster, G. L., Ridgwell, A., Inglis, G. N., Pancost, R. D., Lunt, D. J., & Pearson, P. N. (2016). Changing atmospheric CO2 concentration was the primary driver of early Cenozoic climate. *Nature*, *533*(7603), 380–384. https://doi.org/10.1038/nature17423

Aumont, O., Ethé, C., Tagliabue, A., Bopp, L., & Gehlen, M. (2015). PISCES-v2: An ocean biogeochemical model for carbon and ecosystem studies. *Geoscientific Model Development*, *8*(8), 2465-2513. https://doi.org/10.5194/gmd-8-2465-2015

Baatsen, M., Heydt, A. S. von der, Huber, M., Kliphuis, M. A., Bijl, P. K., Sluijs, A., & Dijkstra, H. A. (2020). The middle-to-late Eocene greenhouse climate, modelled using the CESM 1.0.5. *Climate of the Past Discussions*, 1-44. https://doi.org/10.5194/cp-2020-29

Barker, P. F. (2001). Scotia Sea regional tectonic evolution: Implications for mantle flow and palaeocirculation. *Earth-Science Reviews*, *55*(1-2), 1-39. https://doi.org/10.1016/S0012-8252(01)00055-1

Batenburg, S. J., Voigt, S., Friedrich, O., Osborne, A. H., Bornemann, A., Klein, T., Pérez-Díaz, L., & Frank, M. (2018). Major intensification of Atlantic overturning circulation at the onset of Paleogene greenhouse warmth. *Nature Communications*, *9*(1), 1-8. https://doi.org/10.1038/s41467-018-07457-7

Beerling, D. J., & Royer, D. L. (2011). Convergent cenozoic CO2 history. *Nature Geoscience*, *4*(7), 418–420. https://doi.org/10.1038/ngeo1186

Bice, K. L., Scotese, C. R., Seidov, D., & Barron, E. J. (2000). Quantifying the role of geographic change in Cenozoic ocean heat transport using uncoupled atmosphere and ocean models. *Palaeogeography, Palaeoclimatology, Palaeoecology*, *161*(3–4), 295–310. https://doi.org/10.1016/S0031-0182(00)00072-9

Bijl, P. K., Bendle, J. A. P., Bohaty, S. M., Pross, J., Schouten, S., Tauxe, L., Stickley, C. E., McKay, R. M., Röhl, U., Olney, M., Sluijs, A., Escutia, C., Brinkhuis, H., & Expedition 318 Scientists. (2013). Eocene cooling linked to early flow across the Tasmanian Gateway. *Proceedings of the National Academy of Sciences*, *110*(24), 9645–9650. https://doi.org/10.1073/pnas.1220872110

Bijl, P. K., Schouten, S., Sluijs, A., Reichart, G.-J., Zachos, J. C., & Brinkhuis, H. (2009). Early Palaeogene temperature evolution of the southwest Pacific Ocean. *Nature*, *461*(7265), 776-779. https://doi.org/10.1038/nature08399

Borrelli, C., Cramer, B. S., & Katz, M. E. (2014). Bipolar Atlantic deepwater circulation in the middle-late Eocene: Effects of Southern Ocean gateway openings. *Paleoceanography*, *29*(4), 308–327. https://doi.org/10.1002/2012PA002444

Brinkhuis, H., Schouten, S., Collinson, M. E., Sluijs, A., Damsté, J. S. S., Dickens, G. R., Huber, M., Cronin, T. M., Onodera, J., Takahashi, K., Bujak, J. P., Stein, R., van der Burgh, J., Eldrett, J. S., Harding, I. C., Lotter, A. F., Sangiorgi, F., van Konijnenburg-van Cittert, H., de Leeuw, J. W., Matthiessen, J., Backman, J., Moran, K., & Expedition 302 Scientists. (2006). Episodic fresh surface waters in the Eocene Arctic Ocean. *Nature*, *441*(7093), 606–609. https://doi.org/10.1038/nature04692

Carter, R.M., McCave, I.N., & Carter, L. (2004). Leg 181 synthesis: fronts, flows, drifts, volcanoes, and the evolution of the southwestern gateway to the Pacific Ocean, eastern New Zealand. In Richter, C. (Ed.), Proc. ODP, Sci. Results, 181: College Station, TX (Ocean Drilling Program), 1–111. https://doi.org/10.2973/odp.proc.sr.181.210.2004

Cooke, S., & Rohling, E. J. (1999). Stable oxygen and carbon isotopes in foraminiferal carbonate shells. In B. K. Sen Gupta, *Modern Foraminifera* (pp. 239–258). Springer Netherlands. https://doi.org/10.1007/0-306-48104-9_14

Coxall, H. K., Huck, C. E., Huber, M., Lear, C. H., Legarda-Lisarri, A., O'Regan, M., Sliwinska, K. K., van de Flierdt, T., de Boer, A. M., Zachos, J. C., & Backman, J. (2018). Export of nutrient rich Northern Component Water preceded early Oligocene Antarctic glaciation. *Nature Geoscience*, *11*(3), 190–196. https://doi.org/10.1038/s41561-018-0069-9

Cramer, B. S., Toggweiler, J. R., Wright, J. D., Katz, M. E., & Miller, K. G. (2009). Ocean overturning since the Late Cretaceous: Inferences from a new benthic foraminiferal isotope compilation. *Paleoceanography*, *24*(4). https://doi.org/10.1029/2008PA001683

Cramwinckel, M.J., Huber, M., Kocken, I.J., Agnini, C., Bijl, P.K., Bohaty, S.M., Frieling, J., Goldner, A., Hilgen, F.J., Kip, E.L. & Peterse, F. (2018). Synchronous tropical and polar temperature evolution in the Eocene. *Nature*, *559*(7714), 382-386. https://doi.org/10.1038/s41586-018-0272-2

Cristini, L., Grosfeld, K., Butzin, M., & Lohmann, G. (2012). Influence of the opening of the Drake Passage on the Cenozoic Antarctic Ice Sheet: A modeling approach. *Palaeogeography, Palaeoclimatology, Palaeoecology*, *339–341*, 66–73. https://doi.org/10.1016/j.palaeo.2012.04.023

Dalziel, I. W. D., Lawver, L. A., Norton, I. O., & Gahagan, L. M. (2013). The Scotia Arc: Genesis, Evolution, Global Significance. *Annual Review of Earth and Planetary Sciences*, *41*(1), 767-793. https://doi.org/10.1146/annurev-earth-050212-124155

DeConto, R. M., & Pollard, D. (2003). Rapid Cenozoic glaciation of Antarctica induced by declining atmospheric CO2. *Nature*, *421*(6920), 245–249. https://doi.org/10.1038/nature01290

Donohue, K. A., Tracey, K. L., Watts, D. R., Chidichimo, M. P., & Chereskin, T. K. (2016). Mean Antarctic Circumpolar Current transport measured in Drake Passage. *Geophysical Research Letters*, *43*(22), 11,760-11,767. https://doi.org/10.1002/2016GL070319

Doria, G., Royer, D. L., Wolfe, A. P., Fox, A., Westgate, J. A., & Beerling, D. J. (2011). Declining atmospheric CO2 during the late Middle Eocene climate transition. *American Journal of Science*, *311*(1), 63–75. https://doi.org/10.2475/01.2011.03

Douglas, P. M. J., Affek, H. P., Ivany, L. C., Houben, A. J. P., Sijp, W. P., Sluijs, A., Schouten, S., & Pagani, M. (2014). Pronounced zonal heterogeneity in Eocene southern high-latitude sea surface temperatures. *Proceedings of the National Academy of Sciences*, *111*(18), 6582-6587. https://doi.org/10.1073/pnas.1321441111

Dufresne, J.-L., Foujols, M.-A., Denvil, S., Caubel, A., Marti, O., Aumont, O., Balkanski, Y., Bekki, S., Bellenger, H., Benshila, R., Bony, S., Bopp, L., Braconnot, P., Brockmann, P., Cadule, P., Cheruy, F., Codron, F., Cozic, A., Cugnet, D., … Vuichard, N. (2013). Climate change projections using the IPSL-CM5 Earth System Model: from CMIP3 to CMIP5. *Climate Dynamics*, *40*(9–10), 2123–2165. https://doi.org/10.1007/s00382-012-1636-1

Eagles, G. (2010). South Georgia and Gondwana's Pacific Margin: Lost in translation? *Journal of South American Earth Sciences*, *30*(2), 65-70. https://doi.org/10.1016/j.jsames.2010.04.004

Eagles, G., & Jokat, W. (2014). Tectonic reconstructions for paleobathymetry in Drake Passage. *Tectonophysics*, *611*, 28–50. https://doi.org/10.1016/j.tecto.2013.11.021

Eagles, G., Livermore, R., & Morris, P. (2006). Small basins in the Scotia Sea: The Eocene Drake Passage gateway. *Earth and Planetary Science Letters*, *242*(3-4), 343-353. https://doi.org/10.1016/j.epsl.2005.11.060

Eagles, G., & Scott, B. G. C. (2014). Plate convergence west of Patagonia and the Antarctic Peninsula since 61Ma. *Global and Planetary Change*, *123*, 189-198. https://doi.org/10.1016/j.gloplacha.2014.08.002

Elsworth, G., Galbraith, E., Halverson, G., & Yang, S. (2017). Enhanced weathering and CO2 drawdown caused by latest Eocene strengthening of the Atlantic meridional overturning circulation. *Nature Geoscience*, *10*(3), 213–216. https://doi.org/10.1038/ngeo2888

England, M. H., Hutchinson, D. K., Santoso, A., & Sijp, W. P. (2017). Ice–Atmosphere Feedbacks Dominate the Response of the Climate System to Drake Passage Closure. *Journal of Climate*, *30*(15), 5775-5790. https://doi.org/10.1175/JCLI-D-15-0554.1

Estebenet, M.S.G., Guerstein, G.R. & Alperin, M.I. (2014). Dinoflagellate cyst distribution during the Middle Eocene in the Drake Passage area: paleoceanographic implications. *Ameghiniana*, *51*(6), 500-509. https://doi.org/10.5710/AMGH.06.08.2014.2727

Exon, N. F., Brinkhuis, H., Robert, C. M., Kennett, J. P., Hill, P. J., & Macphail, M. K. (2004). Tectono-sedimentary history of uppermost Cretaceous through Oligocene sequences from the Tasmanian region: A temperate Antarctic margin. In N. F. Exon, J. P. Kennett, & M. J. Malone (Eds.), *Geophysical Monograph Series* (Vol. 151, pp. 319–344). American Geophysical Union. https://doi.org/10.1029/151GM18

Farnsworth, A., Lunt, D. J., O'Brien, C. L., Foster, G. L., Inglis, G. N., Markwick, P., Pancost, R. D., & Robinson, S. A. (2019). Climate Sensitivity on Geological Timescales Controlled by Nonlinear Feedbacks and Ocean Circulation. *Geophysical Research Letters*, *46*(16), 9880-9889. https://doi.org/10.1029/2019GL083574

Fichefet, T., & Morales-Maqueda, M. A. (1997). Sensitivity of a global sea ice model to the treatment of ice thermodynamics and dynamics. *Journal of Geophysical Research: Oceans*, *102*(C6), 12609–12646. https://doi.org/10.1029/97JC00480

Firing, Y. L., Chereskin, T. K., & Mazloff, M. R. (2011). Vertical structure and transport of the Antarctic Circumpolar Current in Drake Passage from direct velocity observations. *Journal of Geophysical Research*, *116*(C8). https://doi.org/10.1029/2011JC006999

Flierdt, T. van de, Frank, M., Halliday, A. N., Hein, J. R., Hattendorf, B., Günther, D., & Kubik, P. W. (2004). Deep and bottom water export from the Southern Ocean to the Pacific over the past 38 million years. *Paleoceanography*, *19*(1). https://doi.org/10.1029/2003PA000923

Frank, M., Whiteley, N., van de Flierdt, T., Reynolds, B. C., & O'Nions, K. (2006). Nd and Pb isotope evolution of deep water masses in the eastern Indian Ocean during the past 33 Myr. *Chemical Geology*, *226*(3–4), 264–279. https://doi.org/10.1016/j.chemgeo.2005.09.024

Galindo-Zaldívar, J., Puga, E., Bohoyo, F., González, F. J., Maldonado, A., Martos, Y. M., Pérez, L. F., Ruano, P., Schreider, A. A., Somoza, L., Suriñach, E., & Antonio, D. de F. (2014). Reprint of "Magmatism, structure and age of Dove Basin (Antarctica): A key to understanding South Scotia Arc development". *Global and Planetary Change*, *123*, 249-268. https://doi.org/10.1016/j.gloplacha.2014.11.002

Gent, P. R., Large, W. G., & Bryan, F. O. (2001). What sets the mean transport through Drake Passage? *Journal of Geophysical Research: Oceans*, *106*(C2), 2693–2712. https://doi.org/10.1029/2000JC900036

Goldner, A., Herold, N., & Huber, M. (2014). Antarctic glaciation caused ocean circulation changes at the Eocene–Oligocene transition. *Nature*, *511*(7511), 574–577. https://doi.org/10.1038/nature13597

Hague, A. M., Thomas, D. J., Huber, M., Korty, R., Woodard, S. C., & Jones, L. B. (2012). Convection of North Pacific deep water during the early Cenozoic. *Geology*, *40*(6), 527–530. https://doi.org/10.1130/G32886.1

Haynes, S. J., MacLeod, K. G., Ladant, J.-B., Guchte, A. V., Rostami, M. A., Poulsen, C. J., & Martin, E. E. (2020). Constraining sources and relative flow rates of bottom waters in the Late Cretaceous Pacific Ocean. *Geology*, *48*(5), 509-513. https://doi.org/10.1130/G47197.1

Hill, D. J., Haywood, A. M., Valdes, P. J., Francis, J. E., Lunt, D. J., Wade, B. S., & Bowman, V. C. (2013). Paleogeographic controls on the onset of the Antarctic circumpolar current. *Geophysical Research Letters*, *40*(19), 5199–5204. https://doi.org/10.1002/grl.50941

Hohbein, M. W., Sexton, P. F., & Cartwright, J. A. (2012). Onset of North Atlantic Deep Water production coincident with inception of the Cenozoic global cooling trend. *Geology*, *40*(3), 255–258. https://doi.org/10.1130/G32461.1

Hollis, C. J., Taylor, K. W. R., Handley, L., Pancost, R. D., Huber, M., Creech, J. B., Hines, B. R., Crouch, E. M., Morgans, H. E. G., Crampton, J. S., Gibbs, S., Pearson, P. N., & Zachos, J. C. (2012). Early Paleogene temperature history of the Southwest Pacific Ocean: Reconciling proxies and models. *Earth and Planetary Science Letters*, *349-350*, 53-66. https://doi.org/10.1016/j.epsl.2012.06.024

Houben, A.J., Bijl, P.K., Sluijs, A., Schouten, S. & Brinkhuis, H. (2019). Late Eocene Southern Ocean cooling and invigoration of circulation preconditioned Antarctica for full-scale glaciation. *Geochemistry, Geophysics, Geosystems*, *20*(5), 2214-2234. https://doi.org/10.1029/2019GC008182

Le Houedec, S., Meynadier, L., & Allègre, C. J. (2016). Seawater Nd isotope variation in the Western Pacific Ocean since 80Ma (ODP 807, Ontong Java Plateau). *Marine Geology*, *380*, 138–147. https://doi.org/10.1016/j.margeo.2016.07.005

Le Houedec, S., Meynadier, L., Cogné, J.-P., Allègre, C. J., & Gourlan, A. T. (2012). Oceanwide imprint of large tectonic and oceanic events on seawater Nd isotope composition in the Indian Ocean from 90 to 40 Ma. *Geochemistry, Geophysics, Geosystems*, *13*(6). https://doi.org/10.1029/2011GC003963

Hourdin, F., Grandpeix, J.-Y., Rio, C., Bony, S., Jam, A., Cheruy, F., Rochetin, N., Fairhead, L., Idelkadi, A., Musat, I., Dufresne, J.-L., Lahellec, A., Lefebvre, M.-P., & Roehrig, R. (2013). LMDZ5B: the atmospheric component of the IPSL climate model with revisited parameterizations for clouds and convection. *Climate Dynamics*, *40*(9–10), 2193–2222. https://doi.org/10.1007/s00382-012-1343-y

Huber, M., Brinkhuis, H., Stickley, C. E., Döös, K., Sluijs, A., Warnaar, J., Schellenberg, S. A., & Williams, G. L. (2004). Eocene circulation of the Southern Ocean: Was Antarctica kept warm by subtropical waters? *Paleoceanography*, *19*(4). https://doi.org/10.1029/2004PA001014

Huber, M., & Caballero, R. (2011). The early Eocene equable climate problem revisited. *Climate of the Past*, *7*(2), 603–633. https://doi.org/10.5194/cp-7-603-2011

Huber, M., Sloan, L. C., & Shellito, C. (2003). Early Paleogene oceans and climate: A fully coupled modeling approach using the NCAR CCSM. In S. L. Wing, P. D. Gingerich, B. Schmitz, & E. Thomas (Eds.), *Causes and Consequences of Globally Warm Climates in the Early Paleogene* (Vol. 369, pp. 25–47). Geological Society of America.

Huck, C.E., van de Flierdt, T., Bohaty, S.M. & Hammond, S.J. (2017). Antarctic climate, Southern Ocean circulation patterns, and deep water formation during the Eocene. *Paleoceanography*, *32*(7), pp.674-691. https://doi.org/10.1002/2017PA003135

Hutchinson, D. K., de Boer, A. M., Coxall, H. K., Caballero, R., Nilsson, J., & Baatsen, M. (2018). Climate sensitivity and meridional overturning circulation in the late Eocene using GFDL CM2.1. *Climate of the Past*, *14*(6), 789–810. https://doi.org/10.5194/cp-14-789-2018

Hutchinson, D. K., Coxall, H. K., Lunt, D. J., Steinthorsdottir, M., de Boer, A. M., Baatsen, M., von der Heydt, A., Huber, M., Kennedy-Asser, A. T., Kunzmann, L., Ladant, J.-B., Lear, C. H., Moraweck, K., Pearson, P. N., Piga, E., Pound, M. J., Salzmann, U., Scher, H. D., Sijp,

W. P., … Zhang, Z. (2020). The Eocene-Oligocene transition: A review of marine and terrestrial proxy data, models and model-data comparisons. *Climate of the Past Discussions*. https://doi.org/10.5194/cp-2020-68

Hutchinson, D. K., Coxall, H. K., O′Regan, M., Nilsson, J., Caballero, R., & de Boer, A. M. (2019). Arctic closure as a trigger for Atlantic overturning at the Eocene-Oligocene Transition. *Nature Communications*, *10*(1), 3797. https://doi.org/10.1038/s41467-019-11828-z

Inglis, G. N., Farnsworth, A., Lunt, D., Foster, G. L., Hollis, C. J., Pagani, M., Jardine, P. E., Pearson, P. N., Markwick, P., Galsworthy, A. M. J., Raynham, L., Taylor, K. W. R., & Pancost, R. D. (2015). Descent toward the Icehouse: Eocene sea surface cooling inferred from GDGT distributions. *Paleoceanography*, *29*(7). https://doi.org/10.1002/2014PA002723

Jakobsson, M., Backman, J., Rudels, B., Nycander, J., Frank, M., Mayer, L., Jokat, W., Sangiorgi, F., O’Regan, M., Brinkhuis, H., King, J., & Moran, K. (2007). The early Miocene onset of a ventilated circulation regime in the Arctic Ocean. *Nature*, *447*(7147), 986–990. https://doi.org/10.1038/nature05924

Katz, M. E., Cramer, B. S., Toggweiler, J. R., Esmay, G., Liu, C., Miller, K. G., Rosenthal, Y., Wade, B. S., & Wright, J. D. (2011). Impact of Antarctic Circumpolar Current Development on Late Paleogene Ocean Structure. *Science*, *332*(6033), 1076–1079. https://doi.org/10.1126/science.1202122

Kennedy-Asser, A. T., Farnsworth, A., Lunt, D. J., Lear, C. H., & Markwick, P. J. (2015). Atmospheric and oceanic impacts of Antarctic glaciation across the Eocene–Oligocene transition. *Philosophical Transactions of the Royal Society A: Mathematical, Physical and Engineering Sciences*, *373*(2054), 20140419. https://doi.org/10.1098/rsta.2014.0419

Kennedy-Asser, A. T., Lunt, D. J., Farnsworth, A., & Valdes, P. J. (2019). Assessing Mechanisms and Uncertainty in Modeled Climatic Change at the Eocene-Oligocene Transition. *Paleoceanography and Paleoclimatology*, *34*(1), 16–34. https://doi.org/10.1029/2018PA003380

Kennett, J. P. (1977). Cenozoic evolution of Antarctic glaciation, the circum-Antarctic Ocean, and their impact on global paleoceanography. Journal of Geophysical Research, 82(27), 3843–3860. https://doi.org/10.1029/JC082i027p03843

Krinner, G., Viovy, N., de Noblet-Ducoudré, N., Ogée, J., Polcher, J., Friedlingstein, P., Ciais, P., Sitch, S., & Prentice, I. C. (2005). A dynamic global vegetation model for studies of the coupled atmosphere-biosphere system. *Global Biogeochemical Cycles*, *19*(1). https://doi.org/10.1029/2003GB002199

Kuhlbrodt, T., Griesel, A., Montoya, M., Levermann, A., Hofmann, M., & Rahmstorf, S. (2007). On the driving processes of the Atlantic meridional overturning circulation. *Reviews of Geophysics*, *45*(2). https://doi.org/10.1029/2004RG000166

Ladant, J.-B., Donnadieu, Y., Bopp, L., Lear, C. H., & Wilson, P. A. (2018). Meridional Contrasts in Productivity Changes Driven by the Opening of Drake Passage. *Paleoceanography and Paleoclimatology*, *33*(3), 302–317. https://doi.org/10.1002/2017PA003211

Ladant, J.-B., Donnadieu, Y., & Dumas, C. (2014a). Links between CO2, glaciation and water flow: reconciling the Cenozoic history of the Antarctic Circumpolar Current. *Climate of the Past*, *10*(6), 1957–1966. https://doi.org/10.5194/cp-10-1957-2014

Ladant, J.-B., Donnadieu, Y., Lefebvre, V., & Dumas, C. (2014b). The respective role of atmospheric carbon dioxide and orbital parameters on ice sheet evolution at the Eocene-Oligocene transition. *Paleoceanography*, *29*(8), 810–823. https://doi.org/10.1002/2013PA002593

Langton, S. J., Rabideaux, N. M., Borrelli, C., & Katz, M. E. (2016). Southeastern Atlantic deep-water evolution during the late-middle Eocene to earliest Oligocene (Ocean Drilling Program Site 1263 and Deep Sea Drilling Project Site 366). *Geosphere*, *12*(3), 1032–1047. https://doi.org/10.1130/GES01268.1

Lefebvre, V., Donnadieu, Y., Sepulchre, P., Swingedouw, D., & Zhang, Z.-S. (2012). Deciphering the role of southern gateways and carbon dioxide on the onset of the Antarctic Circumpolar Current. *Paleoceanography*, *27*(4). https://doi.org/10.1029/2012PA002345

Liu, Z., He, Y., Jiang, Y., Wang, H., Liu, W., Bohaty, S. M., & Wilson, P. A. (2018). Transient temperature asymmetry between hemispheres in the Palaeogene Atlantic Ocean. *Nature Geoscience*, *11*(9), 656–660. https://doi.org/10.1038/s41561-018-0182-9

Liu, Z., Pagani, M., Zinniker, D., DeConto, R., Huber, M., Brinkhuis, H., Shah, S. R., Leckie, R. M., & Pearson, A. (2009). Global Cooling During the Eocene-Oligocene Climate Transition. *Science*, *323*(5918), 1187-1190. https://doi.org/10.1126/science.1166368

Livermore, R., Nankivell, A., Eagles, G., & Morris, P. (2005). Paleogene opening of Drake Passage. *Earth and Planetary Science Letters*, *236*(1-2), 459-470. https://doi.org/10.1016/j.epsl.2005.03.027

Lunt, D. J., Bragg, F., Chan, W.-L., Hutchinson, D. K., Ladant, J.-B., Niezgodzki, I., Steinig, S., Zhang, Z., Zhu, J., Abe-Ouchi, A., de Boer, A. M., Coxall, H. K., Donnadieu, Y., Knorr, G., Langebroek, P. M., Lohmann, G., Poulsen, C. J., Sepulchre, P., Tierney, J., … Otto-Bliesner, B. L. (2020). DeepMIP: Model intercomparison of early Eocene climatic optimum (EECO) large-scale climate features and comparison with proxy data. *Climate of the Past Discussions*. https://doi.org/10.5194/cp-2019-149

Lunt, D. J., Farnsworth, A., Loptson, C., Foster, G. L., Markwick, P., O'Brien, C. L., Pancost, R. D., Robinson, S. A., & Wrobel, N. (2016). Palaeogeographic controls on climate and proxy interpretation. *Climate of the Past*, *12*(5), 1181-1198. https://doi.org/10.5194/cp-12-1181-2016

Lunt, D. J., Huber, M., Anagnostou, E., Baatsen, M. L. J., Caballero, R., DeConto, R., Dijkstra, H. A., Donnadieu, Y., Evans, D., Feng, R., Foster, G. L., Gasson, E., von der Heydt, A. S., Hollis, C. J., Inglis, G. N., Jones, S. M., Kiehl, J., Kirtland Turner, S., Korty, R. L., … Zeebe, R. E. (2017). The DeepMIP contribution to PMIP4: Experimental design for model simulations of the EECO, PETM, and pre-PETM (version 1.0). *Geoscientific Model Development*, *10*(2), 889-901. https://doi.org/10.5194/gmd-10-889-2017

Madec, G. (2008) NEMO ocean engine. Technical note, IPSL, available at http://www.nemo-ocean.eu/content/download/11245/56055/file/NEMO_book_v3_2.pdf

Madec, G., & Imbard, M. (1996). A global ocean mesh to overcome the North Pole singularity. *Climate Dynamics*, *12*(6), 381–388. https://doi.org/10.1007/BF00211684

Marshall, D. P., Munday, D. R., Allison, L. C., Hay, R. J., & Johnson, H. L. (2016). Gill's model of the Antarctic Circumpolar Current, revisited: The role of latitudinal variations in wind stress. *Ocean Modelling*, *97*, 37–51. https://doi.org/10.1016/j.ocemod.2015.11.010

Martin, E. E., & Scher, H. (2006). A Nd isotopic study of southern sourced waters and Indonesian throughflow at intermediate depths in the Cenozoic Indian Ocean. *Geochemistry, Geophysics, Geosystems*, *7*(9). https://doi.org/10.1029/2006GC001302

Maxbauer, D. P., Royer, D. L., & LePage, B. A. (2014). High Arctic forests during the middle Eocene supported by moderate levels of atmospheric CO2. *Geology*, *42*(12), 1027–1030. https://doi.org/10.1130/G36014.1

McKinley, C. C., Thomas, D. J., LeVay, L. J., & Rolewicz, Z. (2019). Nd isotopic structure of the Pacific Ocean 40–10 Ma, and evidence for the reorganization of deep North Pacific Ocean circulation between 36 and 25 Ma. *Earth and Planetary Science Letters*, *521*, 139-149. https://doi.org/10.1016/j.epsl.2019.06.009

Meredith, M. P., Woodworth, P. L., Chereskin, T. K., Marshall, D. P., Allison, L. C., Bigg, G. R., Donohue, K., Heywood, K. J., Hughes, C. W., Hibbert, A., Hogg, A. McC., Johnson, H. L., Jullion, L., King, B. A., Leach, H., Lenn, Y.-D., Morales Maqueda, M. A., Munday, D. R., Naveira Garabato, A. C., … Sprintall, J. (2011). Sustained monitoring of the Southern Ocean at Drake Passage: Past achievements and future priorities. *Reviews of Geophysics*, *49*(4), RG4005. https://doi.org/10.1029/2010RG000348

Mikolajewicz, U., Maier-Reimer, E., Crowley, T. J., & Kim, K.-Y. (1993). Effect of Drake and Panamanian Gateways on the circulation of an ocean model. *Paleoceanography*, *8*(4), 409–426. https://doi.org/10.1029/93PA00893

Munday, D. R., Johnson, H. L., & Marshall, D. P. (2015). The role of ocean gateways in the dynamics and sensitivity to wind stress of the early Antarctic Circumpolar Current. *Paleoceanography*, *30*(3), 284–302. https://doi.org/10.1002/2014PA002675

Najjar, R. G., Nong, G. T., Seidov, D., & Peterson, W. H. (2002). Modeling geographic impacts on early Eocene ocean temperature. *Geophysical Research Letters*, *29*(15), 40-1-40–44. https://doi.org/10.1029/2001GL014438

Nong, G. T., Najjar, R. G., Seidov, D., & Peterson, W. H. (2000). Simulation of ocean temperature change due to the opening of Drake Passage. *Geophysical Research Letters*, *27*(17), 2689–2692. https://doi.org/10.1029/1999GL011072

Pagani, M., Huber, M., Liu, Z., Bohaty, S. M., Henderiks, J., Sijp, W., Krishnan, S., & DeConto, R. M. (2011). The Role of Carbon Dioxide During the Onset of Antarctic Glaciation. *Science*, *334*(6060), 1261–1264. https://doi.org/10.1126/science.1203909

Pagani, M., Huber, M., & Sageman, B. (2014). 6.13 - Greenhouse Climates. In H. D. Holland & K. K. Turekian (Eds.), *Treatise on Geochemistry (Second Edition)* (pp. 281–304). Elsevier. https://doi.org/10.1016/B978-0-08-095975-7.01314-0

Pagani, M., Zachos, J. C., Freeman, K. H., Tipple, B., & Bohaty, S. M. (2005). Marked Decline in Atmospheric Carbon Dioxide Concentrations During the Paleogene. *Science*, *309*(5734), 600–603. https://doi.org/10.1126/science.1110063

Pearson, P. N., Foster, G. L., & Wade, B. S. (2009). Atmospheric carbon dioxide through the Eocene–Oligocene climate transition. *Nature*, *461*, 1110–1113. https://doi.org/10.1038/nature08447

Pearson, P. N., & Palmer, M. R. (2000). Atmospheric carbon dioxide concentrations over the past 60 million years. *Nature*, *406*(6797), 695-699. https://doi.org/10.1038/35021000

Pérez-Díaz, L., & Eagles, G. (2017). South Atlantic paleobathymetry since early Cretaceous. *Scientific Reports*, *7*(1), 1-16. https://doi.org/10.1038/s41598-017-11959-7

Pfister, P. L., Stocker, T. F., Rempfer, J., & Ritz, S. P. (2014). Influence of the Central American Seaway and Drake Passage on ocean circulation and neodymium isotopes: A model study. *Paleoceanography*, *29*(12), 1214–1237. https://doi.org/10.1002/2014PA002666

Rintoul, S. R., Hughes, C., & Olbers, D. (2001). The Antarctic Circumpolar Current system. *In*: Siedler, S., Church, J., Gould, J. (Eds.), Ocean Circulation and Climate, Academic Press, pp. 271–302.

Roberts, C. D., LeGrande, A. N., & Tripati, A. K. (2009). Climate sensitivity to Arctic seaway restriction during the early Paleogene. *Earth and Planetary Science Letters*, *286*(3–4), 576–585. https://doi.org/10.1016/j.epsl.2009.07.026

Sagoo, N., Valdes, P., Flecker, R., & Gregoire, L. J. (2013). The Early Eocene equable climate problem: Can perturbations of climate model parameters identify possible solutions? *Philosophical Transactions of the Royal Society A: Mathematical, Physical and Engineering Sciences*, *371*(2001), 20130123. https://doi.org/10.1098/rsta.2013.0123

Sauermilch, I., Whittaker, J. M., Bijl, P. K., Totterdell, J. M., & Jokat, W. (2019). Tectonic, oceanographic, and climatic controls on the Cretaceous-Cenozoic sedimentary record of the Australian-Antarctic Basin. Journal of Geophysical Research: Solid Earth, 124, 7699–7724. https://doi.org/10.1029/2018JB016683

Scher, H. D., Bohaty, S. M., Zachos, J. C., & Delaney, M. L. (2011). Two-stepping into the icehouse : East Antarctic weathering during progressive ice-sheet expansion at the Eocene–Oligocene transition. *Geology*, *39*(4), 383-386. https://doi.org/10.1130/G31726.1

Scher, H. D., & Martin, E. E. (2004). Circulation in the Southern Ocean during the Paleogene inferred from neodymium isotopes. *Earth and Planetary Science Letters*, *228*(3–4), 391–405. https://doi.org/10.1016/j.epsl.2004.10.016

Scher, H. D., & Martin, E. E. (2006). Timing and Climatic Consequences of the Opening of Drake Passage. *Science*, *312*(5772), 428–430. https://doi.org/10.1126/science.1120044

Scher, H. D., & Martin, E. E. (2008). Oligocene deep water export from the North Atlantic and the development of the Antarctic Circumpolar Current examined with neodymium isotopes. *Paleoceanography*, *23*(1). https://doi.org/10.1029/2006PA001400

Scher, H. D., Whittaker, J. M., Williams, S. E., Latimer, J. C., Kordesch, W. E. C., & Delaney, M. L. (2015). Onset of Antarctic Circumpolar Current 30 million years ago as Tasmanian Gateway aligned with westerlies. *Nature*, *523*(7562), 580–583. https://doi.org/10.1038/nature14598

Sepulchre, P., Arsouze, T., Donnadieu, Y., Dutay, J.-C., Jaramillo, C., Le Bras, J., Martin, E., Montes, C., & Waite, A. J. (2014). Consequences of shoaling of the Central American Seaway determined from modeling Nd isotopes. *Paleoceanography*, *29*(3), 176–189. https://doi.org/10.1002/2013PA002501

Sepulchre, P., Caubel, A., Ladant, J.-B., Bopp, L., Boucher, O., Braconnot, P., Brockmann, P., Cozic, A., Donnadieu, Y., Estella-Perez, V., Ethé, C., Fluteau, F., Foujols, M.-A., Gastineau, G., Ghattas, J., Hauglustaine, D., Hourdin, F., Kageyama, M., Khodri, M., … Tardif, D. (2019). IPSL-CM5A2. An Earth System Model designed for multi-millennial climate simulations. *Geoscientific Model Development Discussions*, 1–57. https://doi.org/10.5194/gmd-2019-332

Sijp, W. P., & England, M. H. (2004). Effect of the Drake Passage Throughflow on Global Climate. *Journal of Physical Oceanography*, *34*(5), 1254–1266. https://doi.org/10.1175/1520-0485(2004)034<1254:EOTDPT>2.0.CO;2

Sijp, W. P., & England, M. H. (2005). Role of the Drake Passage in Controlling the Stability of the Ocean's Thermohaline circulation. *Journal of Climate*, *18*(12), 1957–1966. https://doi.org/10.1175/JCLI3376.1

Sijp, W. P., England, M. H., & Huber, M. (2011). Effect of the deepening of the Tasman Gateway on the global ocean. *Paleoceanography*, *26*(4). https://doi.org/10.1029/2011PA002143

Sijp, W. P., England, M. H., & Toggweiler, J. R. (2009). Effect of Ocean Gateway Changes under Greenhouse Warmth. *Journal of Climate*, *22*(24), 6639–6652. https://doi.org/10.1175/2009JCLI3003.1

Sijp, W. P., von der Heydt, A. S., & Bijl, P. K. (2016). Model simulations of early westward flow across the Tasman Gateway during the early Eocene. *Climate of the Past*, *12*(4), 807–817. https://doi.org/10.5194/cp-12-807-2016

Sijp, W. P., von der Heydt, A. S., Dijkstra, H. A., Flögel, S., Douglas, P. M. J., & Bijl, P. K. (2014). The role of ocean gateways on cooling climate on long time scales. *Global and Planetary Change*, *119*, 1-22. https://doi.org/10.1016/j.gloplacha.2014.04.004

Stärz, M., Jokat, W., Knorr, G., & Lohmann, G. (2017). Threshold in North Atlantic-Arctic Ocean circulation controlled by the subsidence of the Greenland-Scotland Ridge. *Nature Communications*, *8*(1). https://doi.org/10.1038/ncomms15681

Stickley, C. E., Brinkhuis, H., Schellenberg, S. A., Sluijs, A., Röhl, U., Fuller, M., Grauert, M., Huber, M., Warnaar, J., & Williams, G. L. (2004). Timing and nature of the deepening of the Tasmanian Gateway. *Paleoceanography*, *19*(4). https://doi.org/10.1029/2004PA001022

Stoker, M., Leslie, A., Smith, K., Ólavsdóttir, J., Johnson, H., & Laberg, J. S. (2013). Onset of North Atlantic Deep Water production coincident with inception of the Cenozoic global cooling trend: comment. *Geology*, *41*(9). https://doi.org/10.1130/G33670C.1

Tardif, D., Fluteau, F., Donnadieu, Y., Le Hir, G., Ladant, J.-B., Sepulchre, P., Licht, A., Poblete, F., & Dupont-Nivet, G. (2020). *The onset of Asian Monsoons: A modelling perspective* [Preprint]. *Climate of the Past Discussion*. https://doi.org/10.5194/cp-2019-144

Thomas, D. J. (2004). Evidence for deep-water production in the North Pacific Ocean during the early Cenozoic warm interval. *Nature*, *430*(6995), 65-68. https://doi.org/10.1038/nature02639

Thomas, D. J., Korty, R., Huber, M., Schubert, J. A., & Haines, B. (2014). Nd isotopic structure of the Pacific Ocean 70-30 Ma and numerical evidence for vigorous ocean circulation and ocean heat transport in a greenhouse world. *Paleoceanography*, *29*(5), 454-469. https://doi.org/10.1002/2013PA002535

Toggweiler, J. R., & Bjornsson, H. (2000). Drake Passage and palaeoclimate. *Journal of Quaternary Science*, *15*(4), 319–328. https://doi.org/10.1002/1099-1417(200005)15:4<319::AID-JQS545>3.0.CO;2-C

Toggweiler, J. R., & Samuels, B. (1995). Effect of Drake Passage on the global thermohaline circulation. *Deep Sea Research Part I: Oceanographic Research Papers*, *42*(4), 477–500. https://doi.org/10.1016/0967-0637(95)00012-U

Tripati, A., Backman, J., Elderfield, H., & Ferretti, P. (2005). Eocene bipolar glaciation associated with global carbon cycle changes. *Nature*, *436*(7049), 341–346. https://doi.org/10.1038/nature03874

Vahlenkamp, M., Niezgodzki, I., De Vleeschouwer, D., Lohmann, G., Bickert, T., & Pälike, H. (2018). Ocean and climate response to North Atlantic seaway changes at the onset of long-term Eocene cooling. *Earth and Planetary Science Letters*, *498*, 185–195. https://doi.org/10.1016/j.epsl.2018.06.031

Valcke, S. (2006) OASIS3 user's guide (prism-2-5). Tech. Rep. TR/CMGC/06/73, PRISM Report No 3, CERFACS, Toulouse, France

Via, R. K., & Thomas, D. J. (2006). Evolution of Atlantic thermohaline circulation: Early Oligocene onset of deep-water production in the North Atlantic. *Geology*, *34*(6), 441. https://doi.org/10.1130/G22545.1

Wright, N. M., Scher, H. D., Seton, M., Huck, C. E., & Duggan, B. D. (2018). No Change in Southern Ocean circulation in the Indian Ocean from the Eocene through Late Oligocene. *Paleoceanography and Paleoclimatology*, *33*(2), 152–167. https://doi.org/10.1002/2017PA003238

Yang, S., Galbraith, E., & Palter, J. (2014). Coupled climate impacts of the Drake Passage and the Panama Seaway. *Climate Dynamics*, *43*(1–2), 37–52. https://doi.org/10.1007/s00382-013-1809-6

Zachos, J., Pagani, M., Sloan, L. C., Thomas, E., & Billups, K. (2001). Trends, Rhythms, and Aberrations in Global Climate 65 Ma to Present. *Science*, *292*(5517), 686–693. https://doi.org/10.1126/science.1059412

Zhang, X., Prange, M., Steph, S., Butzin, M., Krebs, U., Lunt, D. J., Nisancioglu, K. H., Park, W., Schmittner, A., Schneider, B., & Schulz, M. (2012). Changes in equatorial Pacific thermocline depth in response to Panamanian seaway closure: Insights from a multi-model study. *Earth and Planetary Science Letters*, *317–318*, 76–84. https://doi.org/10.1016/j.epsl.2011.11.028

Zhang, Z.-S., Yan, Q., & Wang, H. (2010). Has the Drake Passage Played an Essential Role in the Cenozoic Cooling? *Atmospheric and Oceanic Science Letters*, *3*(5), 288–292. https://doi.org/10.1080/16742834.2010.11446884

Zhu, J., Poulsen, C. J., & Tierney, J. E. (2019). Simulation of Eocene extreme warmth and high climate sensitivity through cloud feedbacks. *Science Advances*, *5*(9), eaax1874. https://doi.org/10.1126/sciadv.aax1874

6. Figure legends

Figure 1. Eocene bathymetry (40 Ma) used in the different modeling experiments. The red square indicates the Drake Passage (DP) location. It is in a closed configuration (DC) on the global map. The bottom-right figure shows an enlargement of the maximum opening of the DP used in this study (2500 m, D2500).

Figure 2. Global mean annual temperature evolution for the different Eocene experiments at (a) 0 - 10 m, (b) 169 - 238 m, (c) 863 - 1203 m, (d) 2057 - 3012 m and Antarctic Circumpolar Current (ACC) and Antarctic Bottom Water (AABW) evolution through simulation time (e, f). Fluxes are given in Sverdrups (Sv: $10^6 m^3.s^{-1}$). ACC is measured as the transport through the Drake Passage. AABW represents the maximum overturning in the Southern hemisphere deep ocean (below 1500 m).

Figure 3. Annually 0-300 m depth averaged current velocity through the Southern Ocean for DC (a,b) and D2500 (c,d). (c,d) Correspond to qualitative reconstructions of the main water masses present in this area. The dashed lines indicate 40°S and 60°S latitude rings. Abbreviations: BC = Brazil Current; AC = Agulhas Current; WG = Weddell Gyre; RG = Ross Gyre; ACoC = Antarctic Counter Current; EAC = East Australian Current; proto-ACC = proto-Antarctic Circumpolar Current.

Figure 4. Maximum monthly mean value of the mixed layer thickness (m).

Figure 5. Global mean annual meridional stream function in Sverdrup (10^6 $m^3.s^{-1}$) for: (a) DC, (b) D100, (c) D1000, (d) D2500. The blue filled areas denote negative values (anti-clockwise circulation) and the areas filled with warm colors correspond to positive values (clockwise circulation).

Figure 6. Mean annual sea surface temperatures (°C) for (a) DC, and in anomaly with DC for (b) D100, (c) D1000 and (d) D2500.

Figure 7. Latitudinal sea-surface temperature gradient (°C). Bold lines are annual mean values, the thinner lines indicate the highest and lowest annual mean values for a given latitude. Data are late-middle Eocene SST from Tardif *et al*. (2020) after Baatsen *et al*. (2020).

Figure 8. Global mean annual total heat transport (PW: Petawatt = 10^{15} watts). Heat transport is calculated as the sum of latitudinal advective and diffusive transports. Dashed lines indicate anomalies with respect to the DC experiment.

Figure 9. Evolution of the Antarctic climate through the Drake Passage opening.

Figure 10. Mean annual meridional temperatures for: (left column) Pacific Ocean, (middle column) Atlantic Ocean, (right column) Indian Ocean, and from the top to the bottom: DC, D2500 and the anomaly D2500 *minus* DC. The white vertical line represents the equator.

Figure 11. Pressure gradient changes and Surface wind. Globally averaged ocean meridional potential water density (kg/m^3) for (a-d) the different Eocene experiments, (e) modern CTRL experiment and (f) CTRL-4x experiment. The numbers written on each figure correspond to water potential density of this zone. Each line represents a water potential density decrease of 0.1 kg/m^3. The right part of the figure (g) shows the meridional distribution of zonal wind at a 10 m altitude ($m.s^{-1}$) for the different Eocene and modern simulations. Positive values indicate eastward winds, negative values westward winds. Proto-ACC Flow and Modern ACC Flow indicate the maximum strength zone of the ACC in D2500 and CTRL simulations respectively.

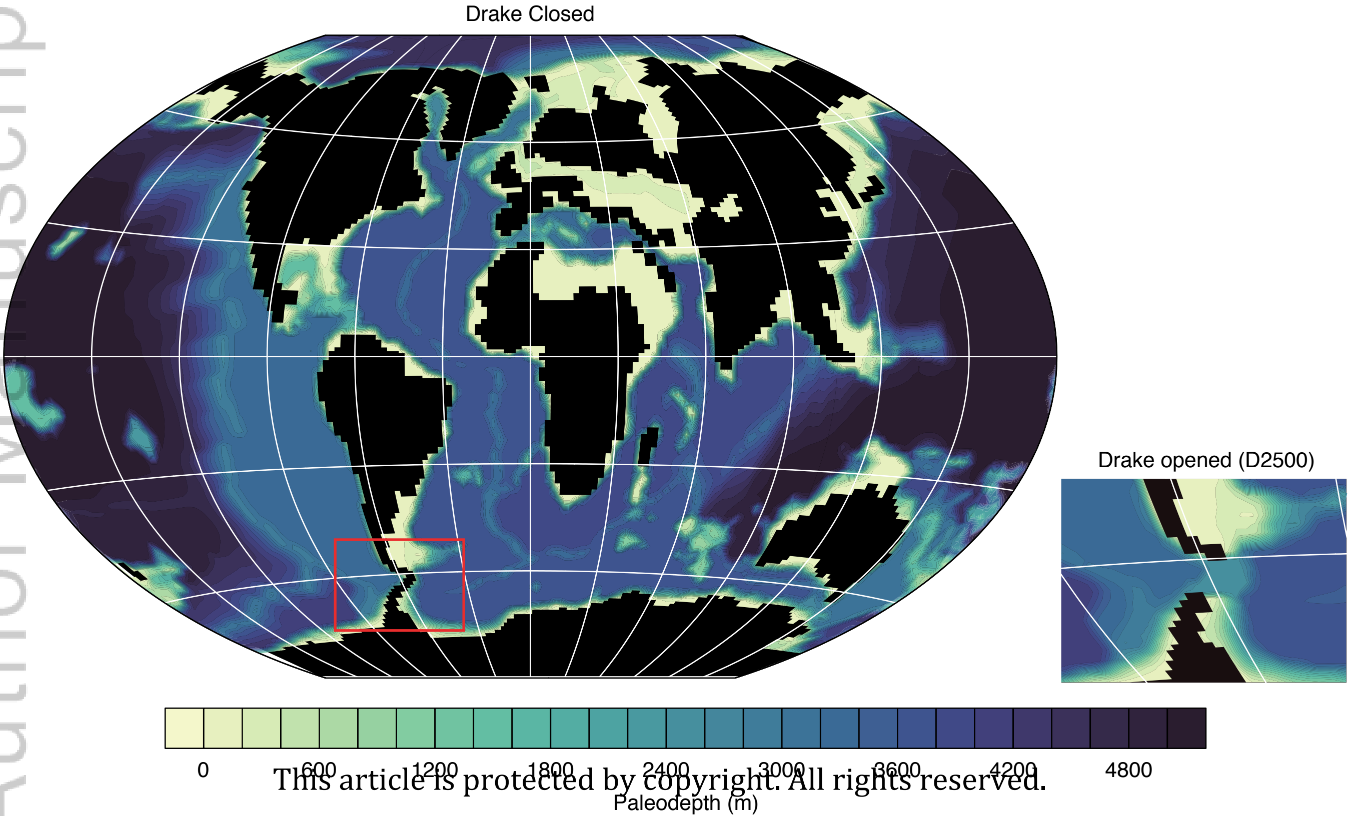
Drake Closed
Drake opened (D2500)
0
600
1200
1800
2400
3000
3600
4200
4800
Paleodepth (m)

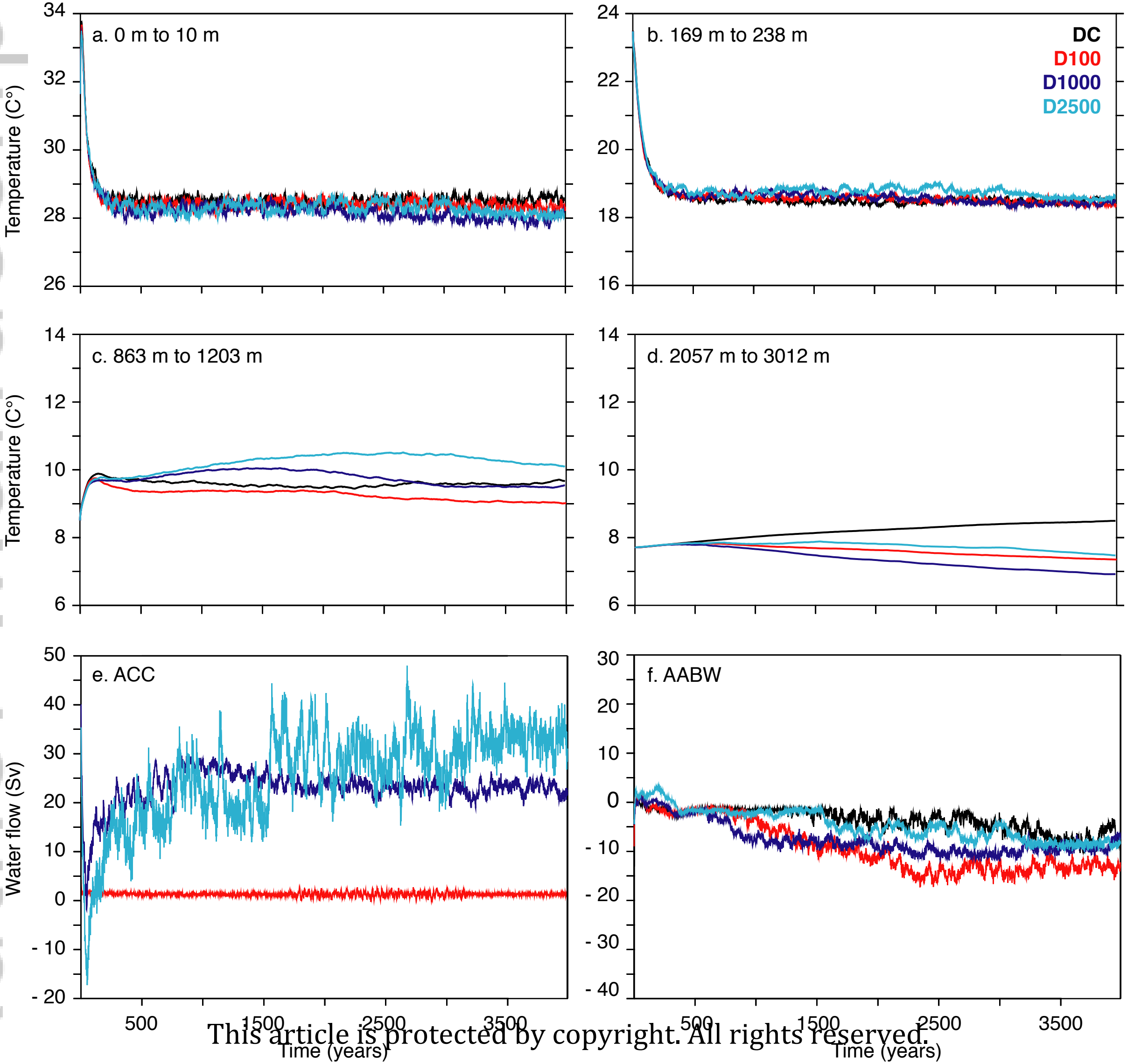
a. 0 m to 10 m
b. 169 m to 238 m
DC
D100
D1000
D2500
c. 863 m to 1203 m
d. 2057 m to 3012 m
e. ACC
f. AABW
Temperature (C°)
Temperature (C°)
Water flow (Sv)
Time (years)
Time (years)
500
1500
2500
3500

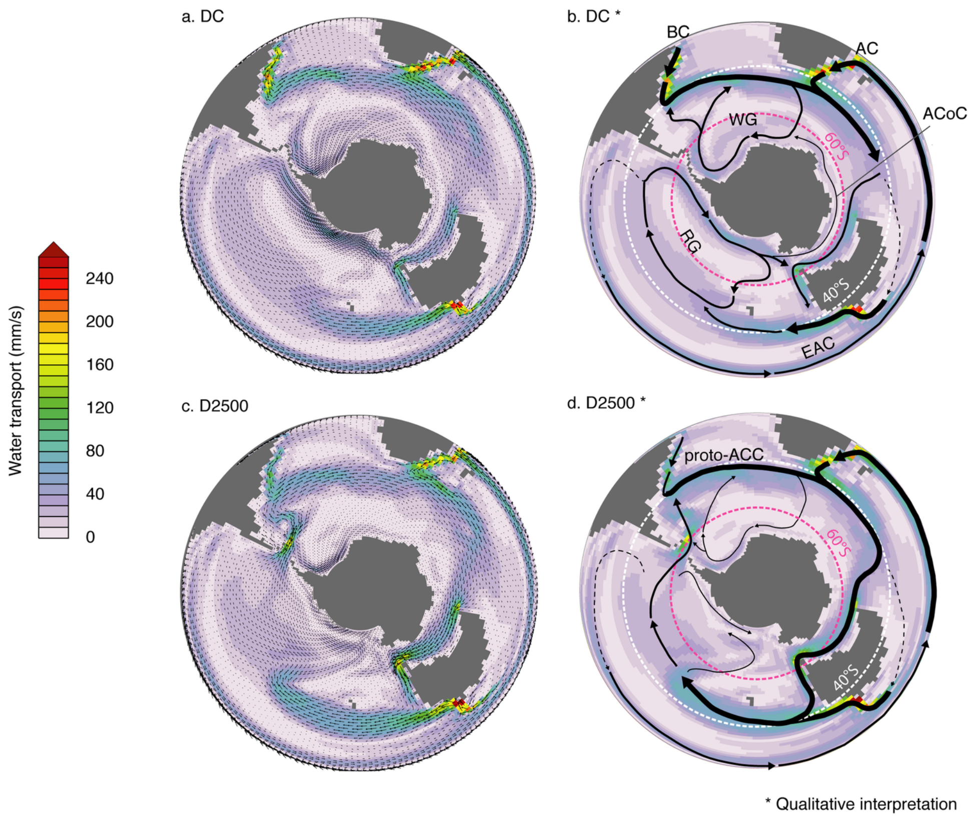

2020PA003889-f03-z-.tif

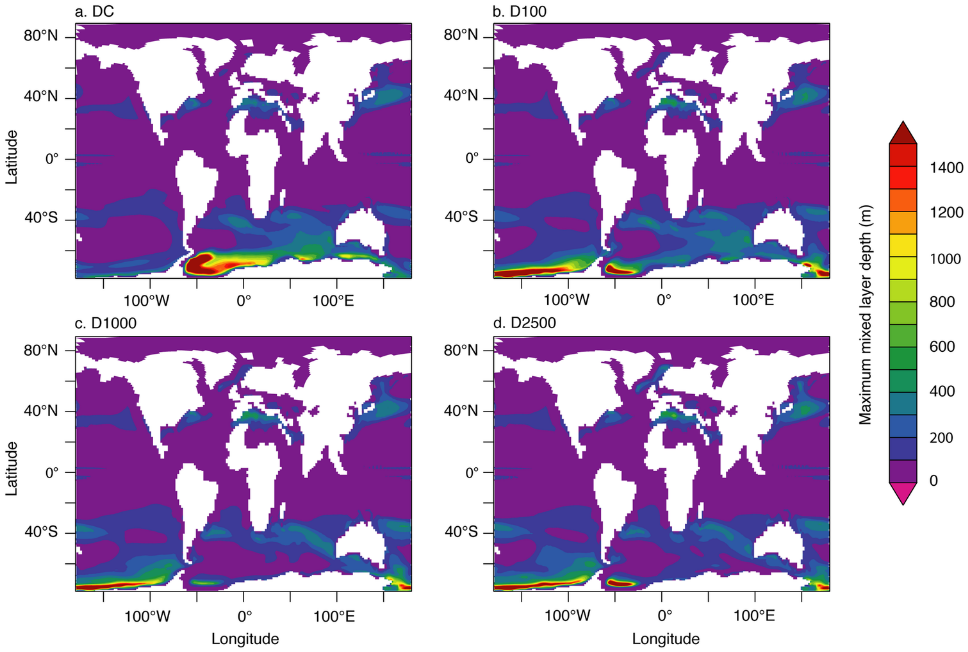

2020PA003889-f04-z-.tif

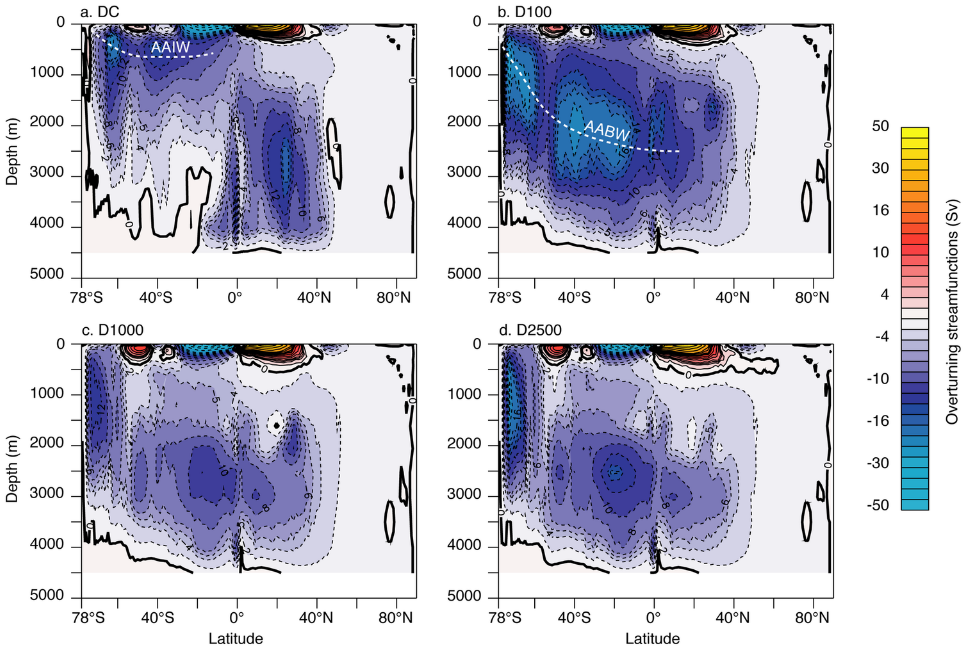

2020PA003889-f05-z-.tif

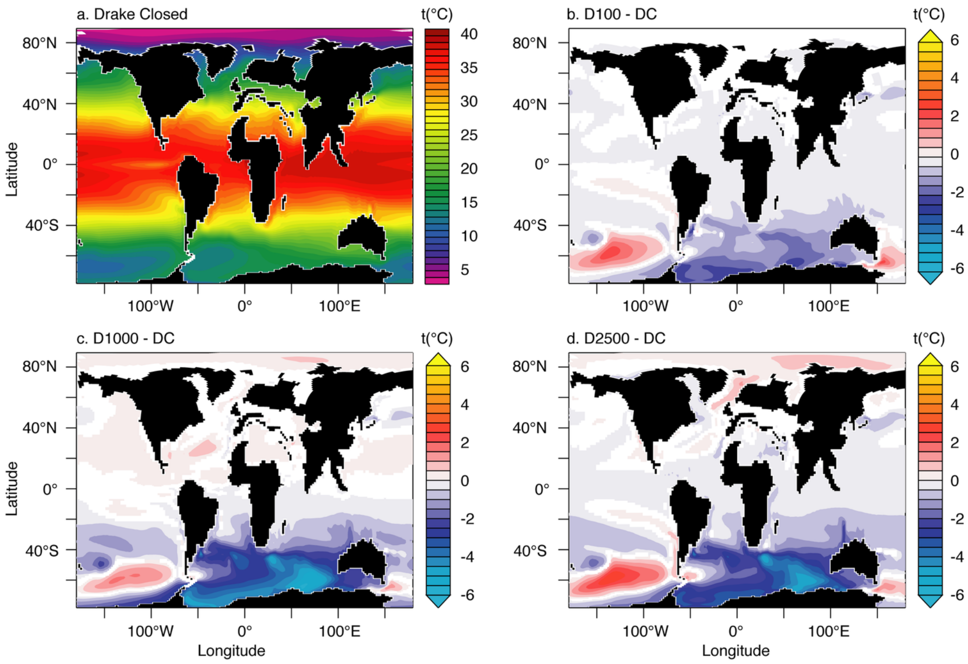

2020PA003889-f06-z-.tif

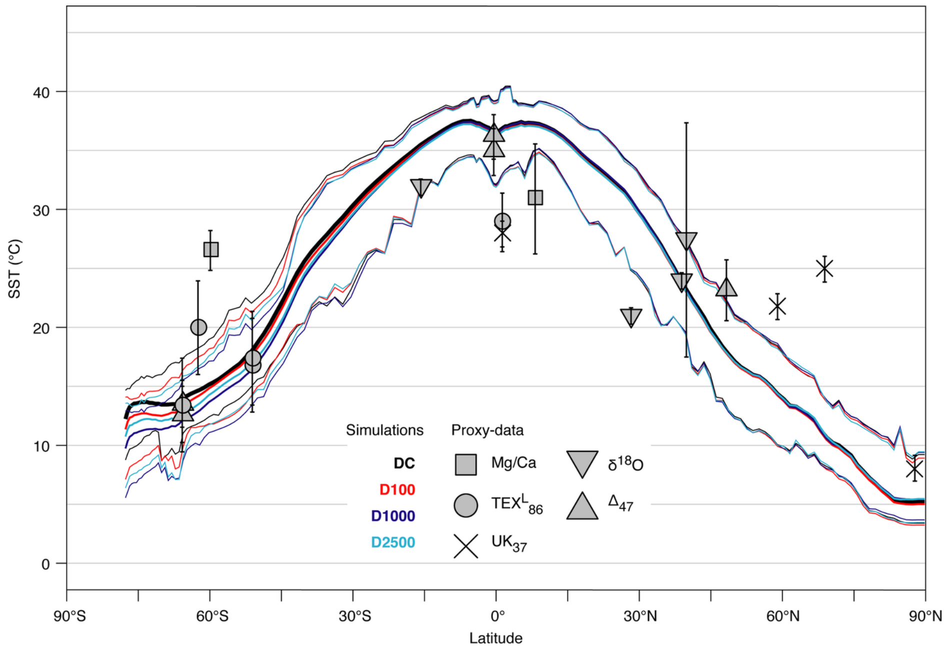

2020PA003889-f07-z-.tif

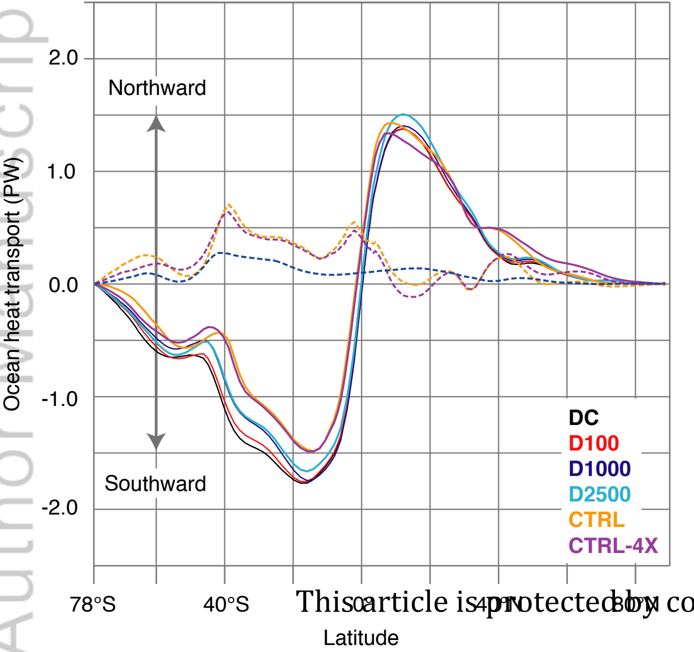
Ocean heat transport (PW)
2.0
1.0
0.0
-1.0
-2.0
Northward
Southward
DC
D100
D1000
D2500
CTRL
CTRL-4X
78°S
40°S
0°
40°N
80°N
Latitude

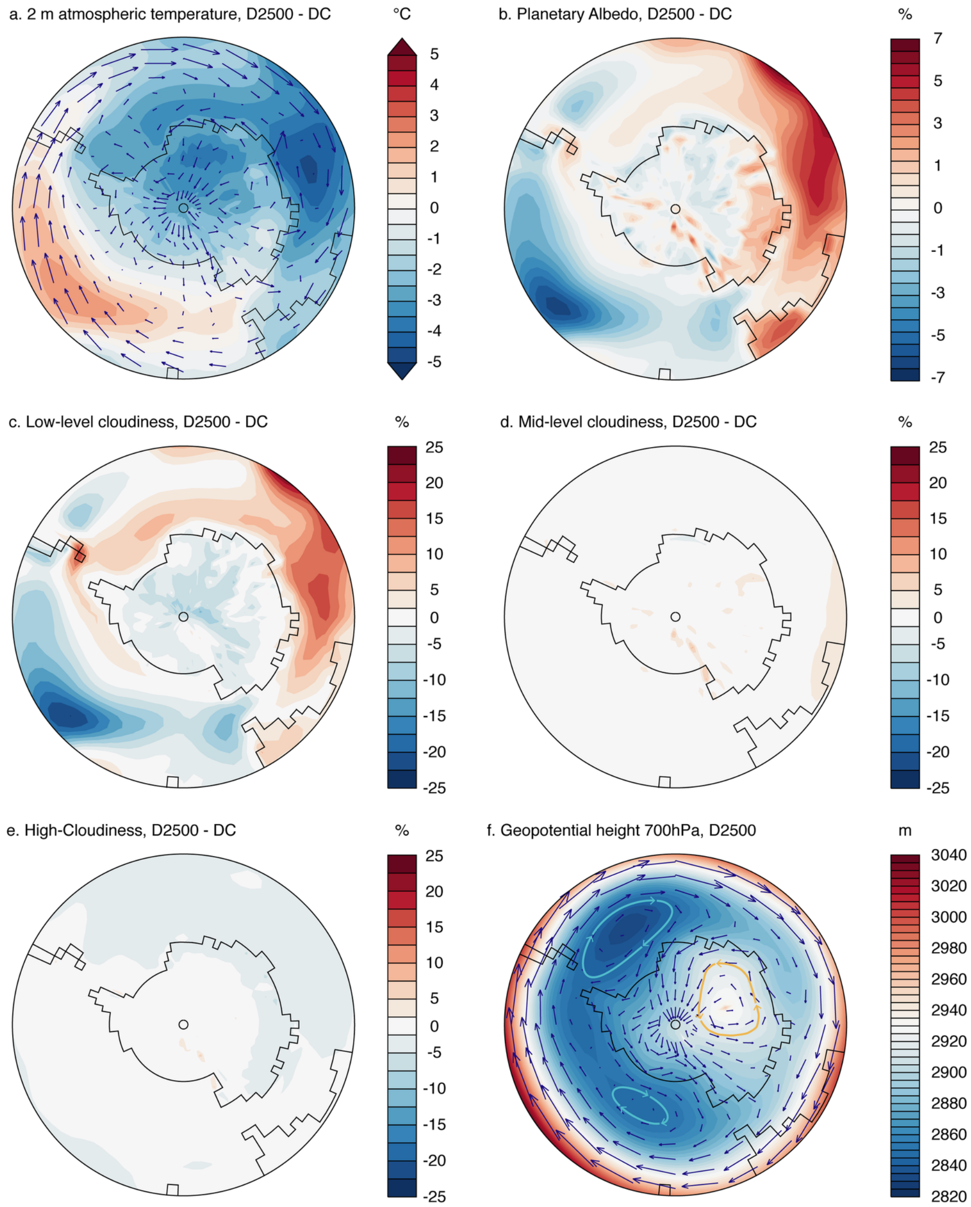

2020PA003889-f09-z-.tif

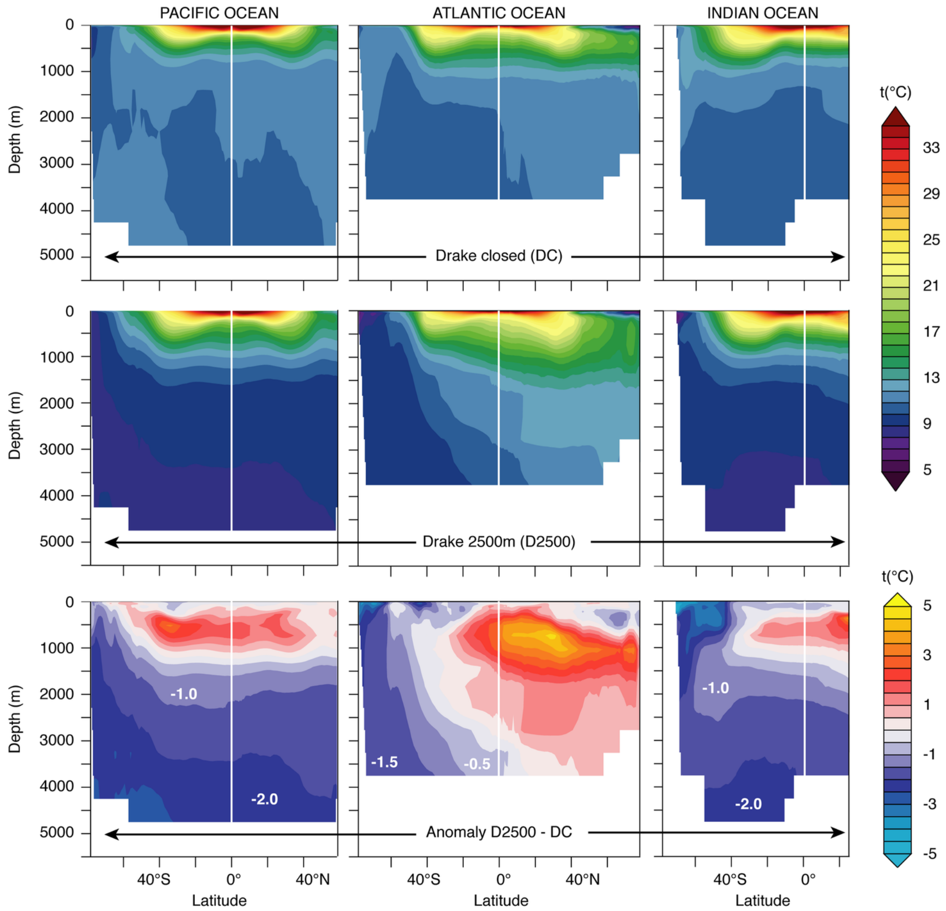

2020PA003889-f10-z-.tif

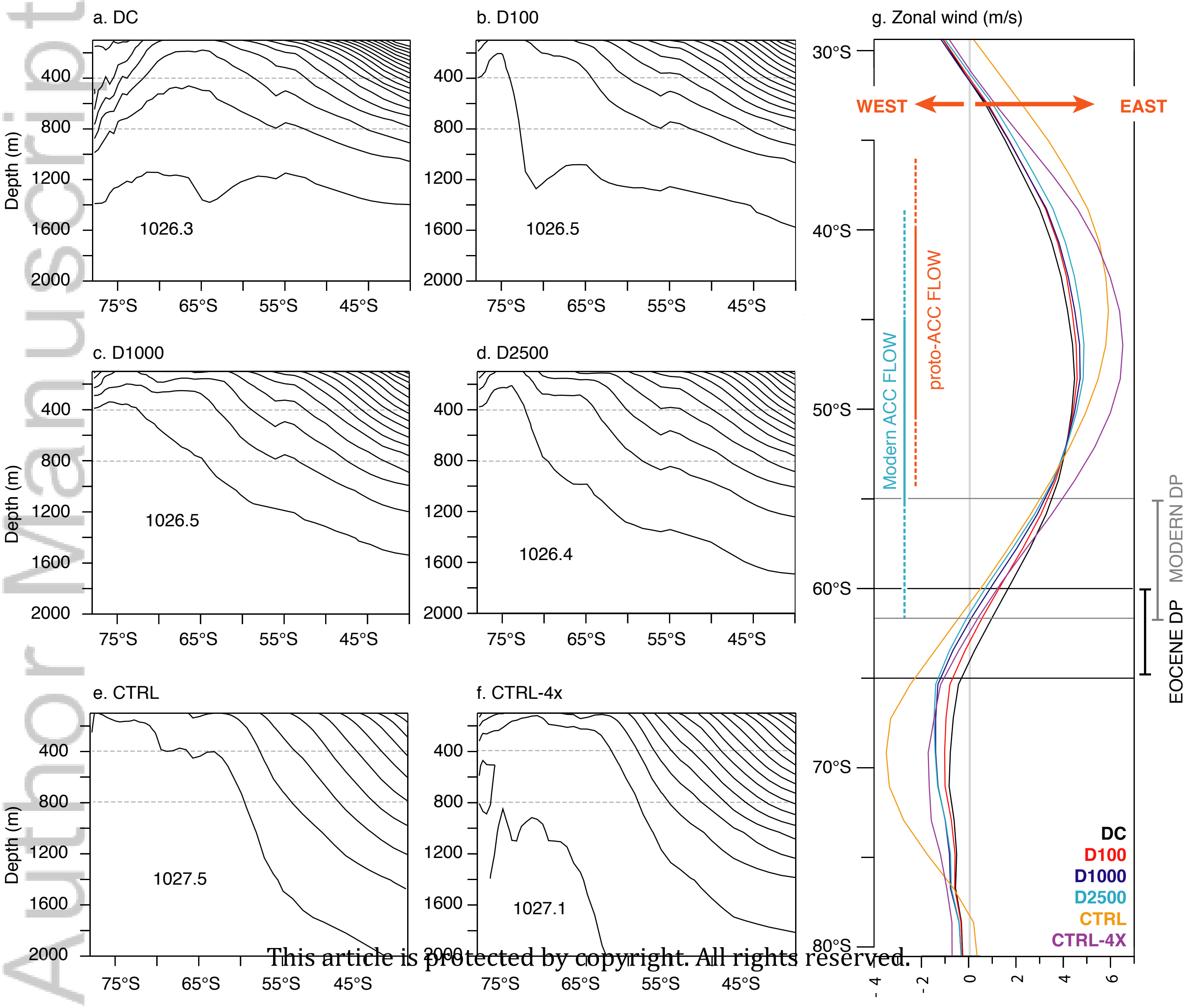

a. DC
b. D100
c. D1000
d. D2500
e. CTRL
f. CTRL-4x
g. Zonal wind (m/s)
Depth (m)
1026.3
1026.5
1026.5
1026.4
1027.5
1027.1
75°S
65°S
55°S
45°S
WEST
EAST
Modern ACC FLOW
proto-ACC FLOW
MODERN DP
EOCENE DP
30°S
40°S
50°S
60°S
70°S
80°S
DC
D100
D1000
D2500
CTRL
CTRL-4X